scientific reports

Check for updates

OPEN

Collision Timing and Provenance Shifts from the Late Oligocene to Middle Miocene in the Southeasternmost Zagros Orogen

Parisa GholamiZadeh[1,6]✉, Bo Wan[1], Eduardo Garzanti[2], Xiumian Hu[3], Rasoul Esmaeili[4] & Mohammad Ebrahimi[5]

Determining the timing of the initial continental collision is a fundamental step in accurately reconstructing the paleogeodynamic evolution of orogenic belts. This process necessitates a comprehensive integration of evidence gathered through various analytical techniques, both in the field and in the laboratory, to achieve a conclusive understanding. We here use comprehensive methods, including sandstone petrography, U-Pb dating, trace element and Hf isotopic compositions of the detrital zircon, in the Haji Abad (eastern Zagros Orogen) and the Shamil areas (west of the Minab-Zendan Fault) to constrain the timing of the initial collision between Arabia and Eurasia. Zircon U-Pb dating in the Haji Abad area reveals that detritus predominantly originates from the Arabia Pan-African basement (~640 – 539 Ma, ε_{Hf} (t): -10 to +10) at the base of the Upper Oligocene-Lower Miocene Razak Formation. This is subsequently replaced up-section by detritus from Cenozoic and Mesozoic Eurasia magmatic-arc sources (~ 54 – 10 Ma, ε_{Hf} (t): -2 to +16; ~110 – 89 Ma, ε_{Hf} (t): -2 to + 20, and ~ 175 – 163 Ma, ε_{Hf} (t): -4 to +10). In contrast, the Shamil area shows that detritus from the Pan-African Arabia basement remained dominant until the Early Miocene. The minimum age of continental collision is characterized by a significant change in provenance, transitioning from detritus sourced from the Arabia lower plate to that derived from the Eurasia upper plate. This transition is documented from the Late Oligocene in the Neyriz and Haji Abad areas along the Main Zagros Thrust, to the Middle Miocene (Langhian) in the Shamil area along the Minab-Zendan Fault.

Keywords Arabia/ Eurasia collision; provenance analysis, Zagros Orogen, Minab-Zendan Fault, Haji Abad and Shamil areas (Iran), Detrital zircon U-Pb dating

Determining the onset of continental collision –defined as the initial contact between opposing continental margins and the initiation of continental subduction– presents a crucial challenge in paleogeodynamic reconstructions. Addressed this challenge requires an integrative approach that combines various field and analytical lines of evidence. One promising approach is provenance analysis of foreland-basin sediments[1–7], which enables us to reconstruct the tectonic and erosional history of newly formed orogenic structures through time. The final disappearance of oceanic lithosphere at one point along the plate boundary, followed by the tectonic growth of the orogenic wedge, marks the onset of continental collision[2,3]. By identifying the first arrival of detritus sourced from the upper plate (Eurasia in this case) in the foreland basin situated on the lower plate (Arabia in this case), we can robustly constrain a minimum age for the onset of collision[2,8–11]. Such an approach not only helps us to constrain the timing of collision but also provides valuable insights into the geodynamic evolution of the orogenic belt during ongoing convergence. In this study, we used a suite of provenance techniques, including sandstone petrography, trace-element geochemistry, U-Pb dating, and Hf

[1]State Key Laboratory of Lithospheric and Environmental Coevolution, Institute of Geology and Geophysics, Chinese Academy of Sciences, Beijing 100029, China. [2]Laboratory of Provenance Studies, Department of Earth and Environmental Sciences, University of Milano-Bicocca, Piazza della Scienza 4, Milano 20126, Italy. [3]Sate Key Laboratory of Critical Earth Material and Mineral Deposits, School of Earth Sciences and Engineering, Nanjing University, Nanjing 210023, China. [4]School of Environmental Sciences, University of East Anglia, Norwich, Norfolk, UK. [5]Department of Geology, Faculty of Sciences, University of Zanjan, Zanjan, Iran. [6]Geological Survey of Iran, Tehran, Iran. ✉email: prsgholami@gmail.com

isotopic composition of detrital zircons. These methods allow us to determine the age distribution of source rocks, the characterize magmatic events in the source region, and track their evolution through time.

The Zagros Orogen, part of the Neotethys suture belt, is bounded to the west by the East Anatolian strike-slip fault in Turkey and separated to the east by the Minab-Zendan Fault from the Makran subduction domain[12]. The timing of collision onset between the Arabia and Eurasia continental margins remains contentious, with various studies proposing different ages based on deformation history[13,14], magmatic episodes[15–18], stratigraphic evolution[19–23], and provenance analysis[5,9–11,24,25]. Based on provenance studies, suggested ages for the onset of continental collision range widely from the Early Miocene in the Bitlis suture zone in Turkey[26–28] to mid-Oligocene in Kurdistan Iraq[10], Late Miocene-Early Pliocene[9], Late Eocene[11], or pre-Eocene[25] in the Lorestan, northwestern Iran; and Pre-Late Oligocene in the Fars region of southeastern Iran[5,24] (Fig. 1a). This variability raises critical questions: Why have different ages been proposed? What are the limitations of provenance studies? Should these findings be reevaluated using tectonostratigraphic data? Was collision time diachronous along the Zagros suture[20,23,29–30] or did it occur relatively synchronously[13]?

The uncertainty about the timing of collision onset and its potential diachroneity along the Zagros suture zone highlights the need for new data to enhance the robustness of provenance interpretations and age determinations across the Zagros orogen. This article aims to address this gap by focusing on the eastern termination of the Zagros orogen –a less tectonically deformed and understudied area connected to the Makran subduction domain. We have integrated provenance and stratigraphic data from the entire Upper Cretaceous-Cenozoic succession, with a specific emphasis on the Upper Oligocene-Lower Miocene Razak Formation. Previous studies have indicated that this lithostratigraphic unit is crucial for constraining the timing of initial continental collision between Arabia and Eurasia[4,5].

Geological background

The Zagros Orogen

The Zagros Fold-Thrust Belt (ZFTB) formed as a consequence of the closure of the Neotethys Ocean and collision between Arabia and Eurasia plates[13]. The Neotethys Ocean opened in front of the northeastern margin of Gondwana following Permian rifting[31–34], which was succeeded by sea-floor spreading during the Triassic period. Since the latest Triassic, the subduction of the Arabia plate beneath Eurasia has facilitated the convergence of these two plates[13,35]. This tectonic interaction has given rise to significant geological features, including the Urumieh-Dokhtar Magmatic Arc (UDMA) and portions of the Sanandaj-Sirjan Zone (SaSZ). Ophiolite obduction in the early Late Cretaceous[36–37] was followed in the Cenozoic by continental collision[13,38], presently propagating eastward toward the Makran domain[39–40].

The Main Zagros Thrust separates the Zagros Fold-Thrust Belt (ZFTB) and remnants of the Neotethys from the Sanandaj-Sirjan Zone, which is part of the Eurasia margin[13,42] (Fig. 1). The ZFTB comprises two geographic provinces –Lorestan and Fars– separated by the Dezful Embayment[13] (Fig. 1a). This belt contains a 12–13 km Eo-Cambrian to Quaternary sedimentary succession accumulated on the northeastern continental margin of Arabia and tectonically accreted to the Eurasia upper plate due to Cenozoic continental collision[13,43] (Fig. 2). The Minab-Zendan Fault, which separates the Zagros orogen from the Makran subduction domain, intersects with the northeastward dipping subduction plane at depth and is connected to the Main Zagros Thrust[41] (Figs. 1 and 2). To the south of the Strait of Hormuz lie the Musandam Peninsula, bordered by the Hagab Fault to the west and the Dibba Fault to the east (Fig. 1). Farther southeast, the Samail Ophiolite, exposed in the northern Oman mountains, was obducted onto the Arabia plate during the early Late Cretaceous (~95 Ma[44–45]).

Magmatism and metamorphism in southeastern Iran

Igneous rocks are widespread to the northeast of the Main Zagros suture, both in the Urumieh-Dokhtar Magmatic Arc and the Sanandaj-Sirjan Zone, which primarily comprises metamorphosed Paleozoic-Mesozoic magmatic-arc and sedimentary rocks[46–47] (Fig. 2). Notable magmatic events in the Sanandaj-Sirjan Zone occurred around 560 Ma (Ediacaran-Cambrian), 330 Ma (Carboniferous), 240 Ma (Triassic), 170 Ma (Middle Jurassic), and 40 Ma (Eocene[13,16,48–52]). Mesozoic calc-alkaline magmatism was closely associated with the subduction of Arabia beneath Eurasia[13,16,50,51,53–55].

The Urumieh-Dokhtar Magmatic Arc, developed to the northeast of the Sanandaj-Sirjan Zone, resulting from ongoing subduction of Arabia beneath Eurasia (Fig. 1, Jebal-e Barez in Fig. 2), primarily consists of calc-alkaline to tholeiitic rocks that formed between 55 and 25 Ma (Eocene-Oligocene)[15–16,51,62–63]. Magmatic activity terminated earlier in the northwest (~22 Ma; Early Miocene) compared to the southeast(~15 – 6 Ma; Middle-Late Miocene)[16].

Permian to Cretaceous sedimentary rocks experienced metamorphism ranging from greenschist-facies to amphibolite-facies during the Jurassic-Cretaceous[13,47,56–58]. These rocks are exposed from the Haji Abad-Esfandagheh (Dowlat-Abad) ophiolitic belt in the northwest to the Upper Jurassic-Lower Cretaceous Bajgan ophiolite-bearing complex in the Makran domain[58] (Fig. 2). The Haji Abad-Esfandagheh region recorded greenschist-facies metamorphism at ~130 – 125 Ma[57], blueschist-facies metamorphism at various intervals between 95 – 85 Ma[47], 106 – 93 Ma, 85 – 80 Ma[59], 85 – 68 Ma[57], and even during the Oligocene[60]. Meta-intrusive rocks in the Bajgan Complex yielded protolith ages of ~161 – 114 Ma[58]. Metapelites with a youngest zircon age of ~ 224 Ma (Triassic[61]) underwent greenschist-facies metamorphism at ~ 100 – 90 Ma[58].

Foreland-basin stratigraphy

In the eastern segment of the Zagros Fold-Thrust Belt, the first sedimentary unit deposited in front of the Neyriz ophiolite after the Late Cretaceous obduction is the Maastrichtian-Paleocene Suchun Formation. This formation comprises sandstone, gypsy marl, and shallow-marine sandy limestone. The unit overlying the Tarbur Limestone transitions to the Jahrum Limestone[43,64–68], which becomes thinner, more evaporitic, and devoid of siliciclastic

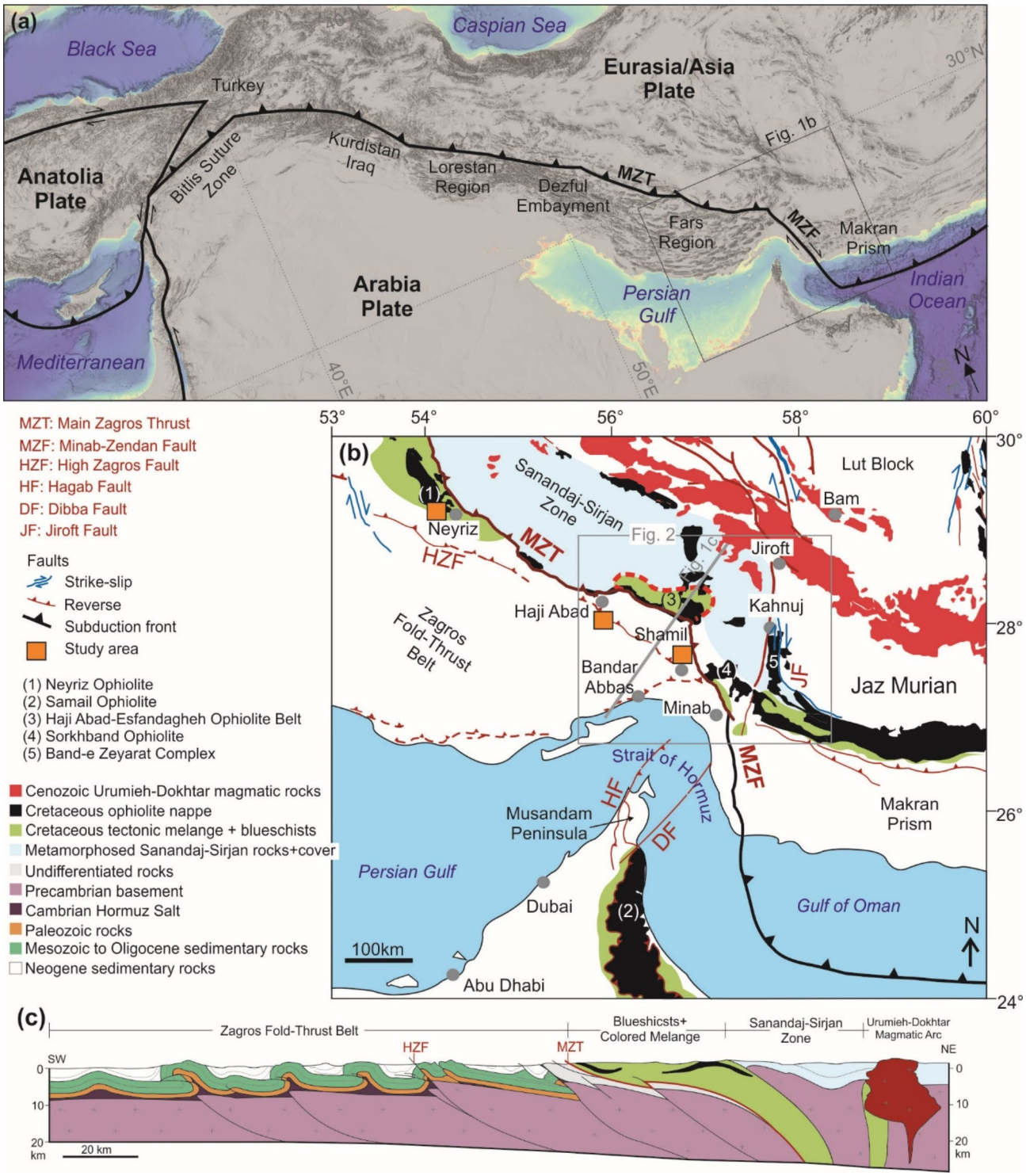

Fig. 1. Location map of the study area. (**a**) The outlined rectangle highlights the study area. (**b**) Haji Abad area, near the Main Zagros Thrust and far from the Neyriz obducted ophiolite, and Shamil area close to the Minab-Zendan Fault at the terminus of the Arabia- Eurasia suture (modified[47]). (**c**) A cross-section from the UDMA to the Persian Gulf, as illustrated in Fig. 1b (modified[47]). The map was modified by GholamiZadeh, P. using CorelDraw x8 v.16 software (http://www.coreldraw.com/en/product/coreldraw).

detritus away from the obducted Neyriz ophiolite[43,53] (Fig. 3). The Suchun Formation distally grades into the deep-marine marls and marly limestones of the Pabdeh Formation toward the southeast (Fig. 3). This latter unit overlies pelagic marls of the Gurpi Formation, close to the Mianb-Zendan Fault[67] (Fig. 3). The Jahrum Limestone is extensively distributed across the eastern Zagros, having been deposited during an early-middle Eocene sea-level rise[69]. It is unconformably overlain by interbedded red mudrocks and sandstones of the Razak Formation

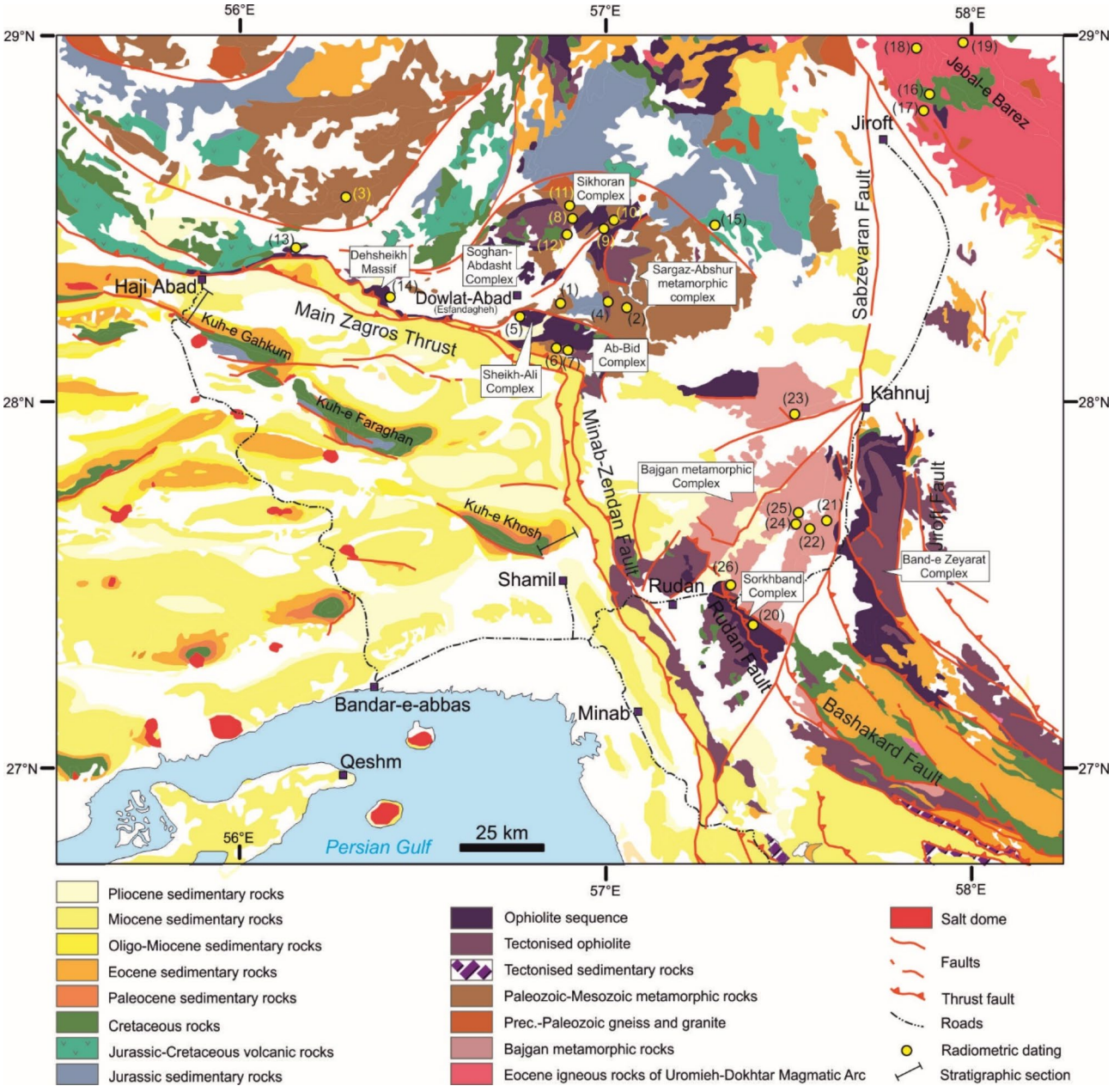

Fig. 2. Geological map of the eastern Zagros Fold-Thrust Belt (modified[124]). The Minab-Zendan dextral thrust fault delineates the Zagros collisional domain from the Makran subduction domain. The Main Zagros Thrust separates Zagros Fold-Thrust Belt (Arabia lower plate) from the Sanandaj-Sirjan metamorphic belt (Eurasia upper plate). Radiometric ages provided include: (1) 188 Ma, (2) 318 Ma, and (3) 546 Ma (U-Pb dating of metamorphic rocks[57]); (4) 186 Ma and (5) 174 Ma (U-Pb dating of ophiolites[57]); (6) 117 Ma, (7) 102 – 87 Ma, (8) 126 – 95 Ma, (9) 109 – 89 Ma, (10) 102 – 82 Ma, (11), and (12) 85 – 80 Ma (Ar-Ar dating of blueschists[47,59]); (13) 91 Ma, (14) 87 and 90 Ma (U-Pb dating of dacite and plagiogranite, respectively[85]); (15) 175 Ma, (16) 77 Ma, (17) 31 – 29 Ma (18) 45 Ma, and (19) 20 – 18 Ma, (U-Pb dating of igneous rocks[16]); (20) 476 Ma (K-Ar dating of clinopyroxenite[125]); (21) 137 Ma, (22) 119 Ma, and (23) 156 Ma (U-Pb dating of metavolcanic rocks[59]); (24) 91 Ma, (25) 100 Ma, and (26) 94 Ma (Ar-Ar dating of greenschists[59]). The map was modified by GholamiZadeh, P. using CorelDraw x8 v.16 software (http://www.coreldraw.com/en/product/coreldraw).

along the Main Zagros Thrust. This regional unconformity, which spans from the late Eocene to Oligocene, may be attributed to flexural uplift of a fore-bulge[23,54] associated with fold deformation and exposure of the underlying succession[69–70]. The Razak Formation is overlain by the marly limestones of the basal Guri Member of the Mishan Formation[71–72]. The Guri limestone transitions into shallow-marine marl and sandstone of the upper Mishan Formation, which is in turn overlain by red mudrocks and sandstones of the Aghajari Formation.

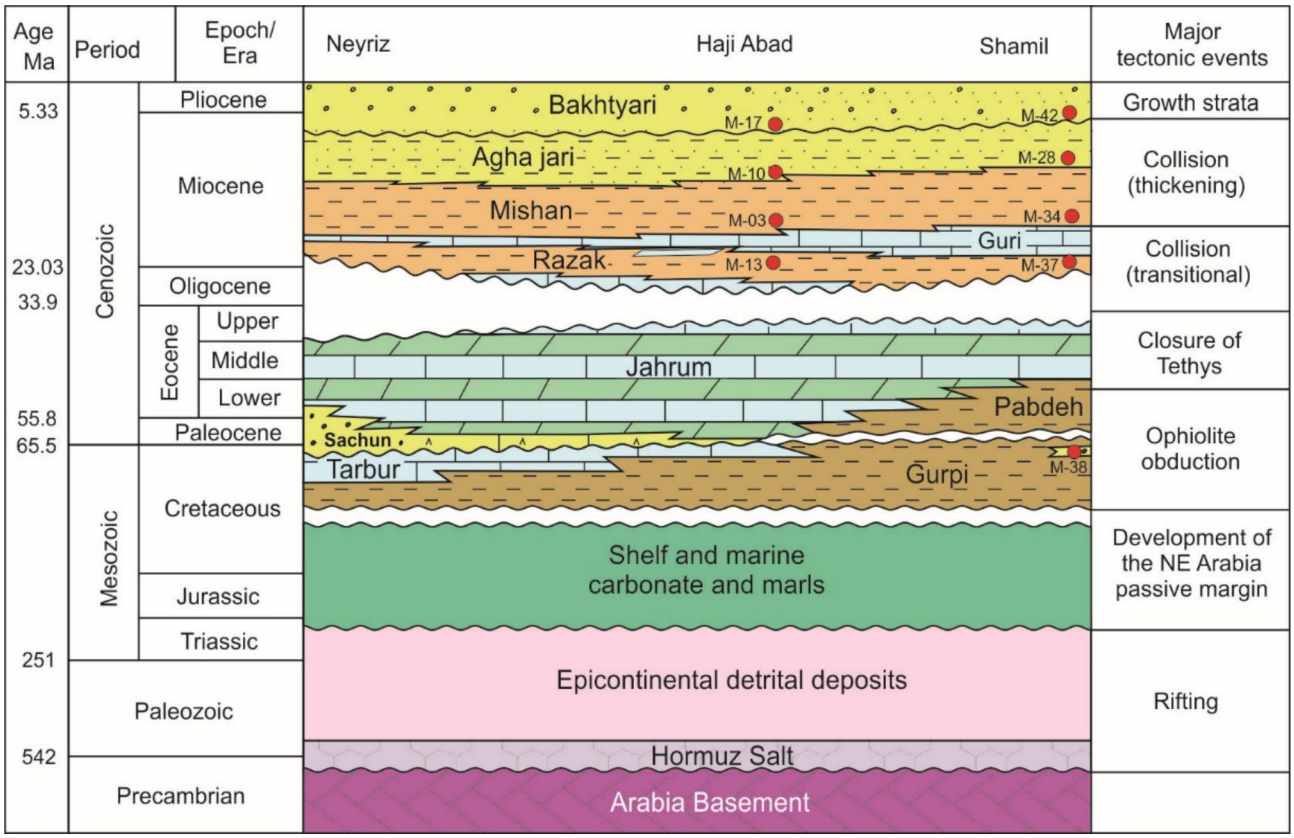

Fig. 3. Stratigraphic framework for the eastern Zagros Fold-Thrust Belt (based on own data and Piryaei et al.[67–68]. It highlights the differences in Upper Cretaceous-Paleocene facies as well as the Late Eocene-Oligocene hiatus across the eastern Zagros Fold-Thrust Belt. Red dots indicate stratigraphic positions of samples used for U-Pb zircon dating.

Ultimately, the Zagros foreland basin was filled with conglomerates of the Pliocene Bakhtyari Formation[64,73] (Fig. 3).

Ophiolite complexes in the eastern Zagros

The study are features several ophiolite remnants, including the Neyriz, Haji Abad-Esfandagheh, and Rudan-Sorkhband complexes in Iran, as well as the Samail ophiolite in Oman (Fig. 1). Both Neyriz and Samail ophiolites were obducted onto the Arabia plate during the early Late Cretaceous[13,36,44]. Zircon U-Pb dating of igneous rocks associated with the Neyriz ophiolite suggests that it was emplaced at 100 – 93 Ma in a fore-arc setting[74–76]. Similarly, the Samail ophiolite of 96 – 94 Ma exhibits its formation in a supra-subduction setting[45,77–79]. The Haji Abad-Esfandagheh (Dowlat-Abad) ophiolitic belt is exposed along the Main Zagros Thrust, north of Haji Abad town. This belt comprises various ophiolitic bodies (Figs. 1 and 2) that have thrust together with associated mélanges and Paleozoic metamorphic rocks onto Eocene-Oligocene turbidities within the Sanandaj-Sirjan Zone[47,80]. Two distinct groups of ophiolite bodies have been identified. The first group consists of Jurassic Soghan-Abdasht and Sikhoran bodies dated as 174–186 Ma[57,81], and are embedded within Paleozoic-Mesozoic rocks and overlain by Jurassic-Cretaceous strata[60] (Fig. 2). They are considered to have formed in either back-arc[82,83] or rift[57,84] settings. In contrast, the second group comprises Cretaceous Haji Abad, Sheikh-Ali, Dehsheikh, Ab-Bid bodies, which are exposed near the Main Zagros Thrust, dated at 87–91 Ma and have originated in a fore-arc setting[84–85](Fig. 2). A MORB-supra subduction origin has been indicated for the Ab-Bid ultramafic complex, which is associated with Cretaceous radiolarite[86]. Additionally, several ophiolitic complexes are present in the Makran domain (Fig. 2). The Sorkband ophiolite exposed to the east of the Minab-Zendan Fault is considered to have formed in a MORB-supra subduction setting during the Cretaceous[18,87]. Meta-ophiolitic rocks within the Bajgan Complex were dated as 116 – 114 Ma[58].

Samples and methods

To constrain the timing of continental collision in the eastern Zagros Fold-Thrust Belt, We focused on three main areas: (i) the Neyriz area, serving as a reference for ophiolite obduction (Rowshan Kuh section); (ii) the Haji Abad area (west of the Kuh-e Gahkum anticline) at the structural terminus of the Zagros Crush Zone; and (iii) the Shamil area (east of the Kuh-e Khosh anticline), being closest to the Minab-Zendan Fault (detailed location information can be found in Supplementary Table S1, Figs. 1 and 2). Our investigation included new biostratigraphic and provenance studies on Upper Cretaceous to Pliocene strata in both the Haji Abad and

Shamil areas (Fig. 3), whereas the provenance study for the Neyriz area is detailed in GholamiZadeh et al.[4,5]. We specifically sampled from the Upper Cretaceous sediments, where the initial arrival of ophiolite detritus has been previously documented[69].

- During our field surveys in the Haji Abad and Shamil areas, we collected a total of 25 medium-grained sandstone samples for petrographic analysis, six limestone samples for biostratigraphic analysis, and nine samples for rare-earth-element (REE) analysis, and combined U-Pb and Hf isotopic analyses of detrital zircons. These samples were systematically collected from continuous stratigraphic sections, both below and above unconformities and facies discontinuities. For petrographic analysis, 300 grains were point-counted by the Gazzi-Dickinson's method[88–89] (Supplementary Table S2), with a specific focus on identifying lithic grain types[90–92]. Sandstone classification followed after Garzanti's methodology[93,94].
- Heavy minerals were separated using traditional washing techniques, and ~120 zircon grains were randomly hand-picked from each sample and mounted in epoxy resin. Cathodoluminescence images were used to accurately position the laser spot, ensuring that rims and inclusions were avoided. U-Pb and REE analyses were conducted simultaneously using the ESI New Wave NWR 193^{UC} (TwoVol2) laser ablation system connected to an Agilent 8900 ICP–QQQ in the Beijing Quick-Thermo Science & Technology Co., Ltd, China. The operational parameters included a 25-µm-diameter beam, ~4 J/cm^2 fluence, and a 5 Hz repetition rate. Zircon U-Pb and REE data were processed by Iolite data reduction software[95] (https://iolite.xyz), while histograms of U-Pb zircon ages were generated using Density plotter 8.5[96] (https://www.ucl.ac.uk/~ucfbpve/densityplotter) (Supplementary Table S3-4).
- For combined U-Pb and Hf isotopic analysis of detrital zircons, we selected four samples that spanned the Upper Cretaceous-Pliocene stratigraphic range. These analyses were preformed using a Neptune (Plus) MC-ICP-MS (Thermo Fisher Scientific, USA), equipped with an Analyte G2 193 nm ArF excimer laser ablation system at the Institute of Geology and Geophysics, Chinese Academy of Sciences in Beijing, China. The operational conditions included a 65-µm spot size, 5 J/cm^2 fluence, and a 6 Hz repetition rate. Data correction was carried out during and after analysis following established protocols[97–100] (Supplementary Table S5).

Results

Stratigraphy

Upper cretaceous-Lower Eocene strata In the Haji Abad area, the Upper Cretaceous-Paleocene interval is represented by the ~80 m-thick Sachun Formation. This unit, overlying the Maastrichtian Tarbur Formation and followed by the Jahrum Limestone (Fig. 4-a,), consists of gypsiferous limestone, dolomite, marl, marly limestone, and peloidal grainstone (Figs. 3 and 4-a and b) lacking siliciclastic detritus and age-diagnostic fossils (Fig. 4-c). In the Neyriz area, the Sachun Formation reaches a thickness of ~200 m and contains clasts of radiolarite and serpentinite.

In the Shamil area (Kuh-e Khosh), the Upper Cretaceous-Lower Eocene interval is 1400 m-thick and consists of gray pelagic marls interbedded with thin layers of marly limestones of the Gurpi and Pabdeh formations (Fig. 4-d, e). The Santonian to Maastrichtian Gurpi Formation[67] is unconformably overlain by the Middle Paleocene (Selandian) to Eocene Pabdeh Formation, which consists of marly limestone, limestone, and marl[101]. The Gurpi Formation includes abundant planktonic foraminifera in the lower part and ~2 m of slumped conglomerate with boulders of basalt, diabase, and rhyolitic tuffs near the top (Fig. 4-d, e). Previously reported blocks of ultramafic rocks[67,102] were not observed during our study.

Upper Oligocene-Lower Miocene Razak Formation In the Haj Abad and Neyriz areas, the 200-m-thick Razak Formation unconformably overlies the Early to Middle Eocene Jahrum Formation and is overlain by the Lower Miocene (Burdigalian) Guri Member of the Mishan Formation (Figs. 3 and 4-f). The Razak Formation mainly consists of red mudrock and sandstone, with intercalated gypsiferous sandy limestone and mainly matrix-supported conglomerate featuring well-rounded clasts with medium to high sphericity (Fig. 4-f-j). Quartz and limestone rock fragments are common in the basal part of the unit, whereas radiolarite, serpentinite, and igneous rock fragments become more prevalent toward the top. A limestone interval at the base of the Razak Formation in the Haji Abad area contains Oligocene microfossils (*Eulepidina dilatata*, *Archaias* sp., *Neorotalia* sp., *Austrotrillina*, sp., *Quinqueloculina* sp.) that were not found in the Neyriz and Shamil areas.

In contrast, the 50-m-thick Razak Formation in the Shamil area consists of alternating yellowish-gray sandstone and red mudrock overlying the Eocene Jahrum Formation (Fig. 4-f, h). The clasts are predominantly quartz, with carbonate grains commonly containing reworked Paleocene-Early Oligocene foraminifera (*Nummulites fichteli*, *N. vascus*, *N. intermedius*, *Amphistegina* sp., *Neoalveolina* sp.).

Lower-Middle Miocene Mishan Formation The Mishan Formation consists of green and gray marl with sandy limestone and sandstone layers overlain by the lower Serravallian (?) Aghajari Formation (Fig. 5-a, b). The cream-colored reefal limestone of the basal Guri Member (Fig. 5-a) –Early Miocene (Burdigalian) in age based on the foraminifera *Elphidium* sp., *Neoalveolina melo-curdica*, *Taberina malabarica*, *Operculina sp.*, *Miogypsina sp.*, and *Meandropsina sp.* – is replaced up-section by green marls with thin interbedded limestone, suggesting deposition in open shallow-marine environments (Fig. 5-a). The thickness of the Mishan Formation increases from 300 m in the Neyriz area to 1100 m in the Haji Abad area, and reaching up to ~2500 m in the Shamil area.

Middle-Upper Miocene Aghajari Formation The unfossiliferous Aghajari Formation lies above the Langhian strata of the Mishan Formation[101] and is unconformably overlain by the Bakhtyari Formation. This formation primarily consists of red mudrock and sandstone, with thickening from ~400 m in the Neyriz area to ~2000 m

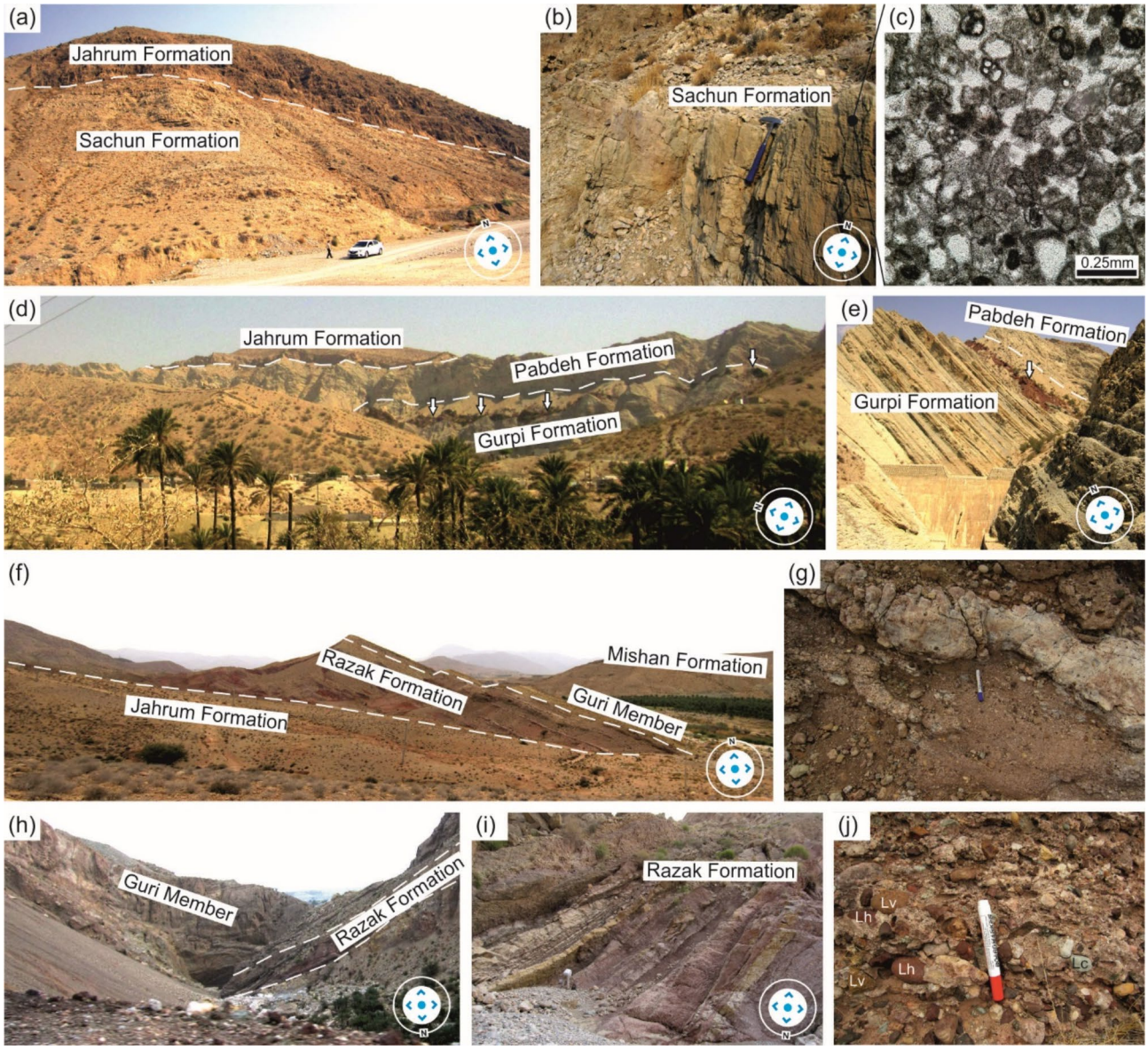

Fig. 4. Upper Cretaceous to Miocene stratigraphy: (**a**, **b**) The Upper Cretaceous-Paleocene Sachun Formation is overlain by the Eocene Jahrum Formation in the Haji Abad area. (**c**) A Peloidal bioclastic grainstone from the Sachun Fm. notable for its lack of siliciclastic detritus. (**d, e**) The Upper Cretaceous-Paleocene Gurpi and Pabdeh formations, which are capped by the Eocene Jahrum Limestone in the Shamil area. Arrows in (**d**) and (**e**) highlight a 2-m-thick red-purple slumped conglomerate near top of Gurpi Formation. The Razak Fm. is limited between the Jahrum Fm. and Guri Member in the Haji Abad area (**f**) and Shamil area (**h**). (**g**) A gypsum layer in the Razak Fm. (Haji Abad area). (**i**) Alternating yellowish-gray sandstone and red mudrock of the Razak Fm. in the Shamil area. (**j**) Radiolarite, and limestone pebbles in conglomerate of Razak Fm. in the Haji Abad area. Abbreviations as in Fig. 6.

in the Haji Abad area and up to ~3900 m in the Shamil area (Fig. 5-b, c). The geometry of sandstone and conglomerate beds transitions from tabular at the base to lenticular at the top, indicating a fluvial depositional environment (Fig. 5-c, d).

Upper Miocene-Pliocene Bakhtyari Formation The Bakhtyari Formation exhibits a thickness that increases from ~300 m in the Neyriz area to <1000 m in the Haji Abad area and up to 3900 m in the Shamil area. This formation is characterized by well-cemented, moderately sorted, sheet-like pebbly to cobbly conglomerates, which predominantly contain clasts derived from Cretaceous carbonate, radiolarian chert, and volcanic rocks. The evidence suggests that deposition occurred in alluvial fan to fluvial settings (Fig. 5-e-f).

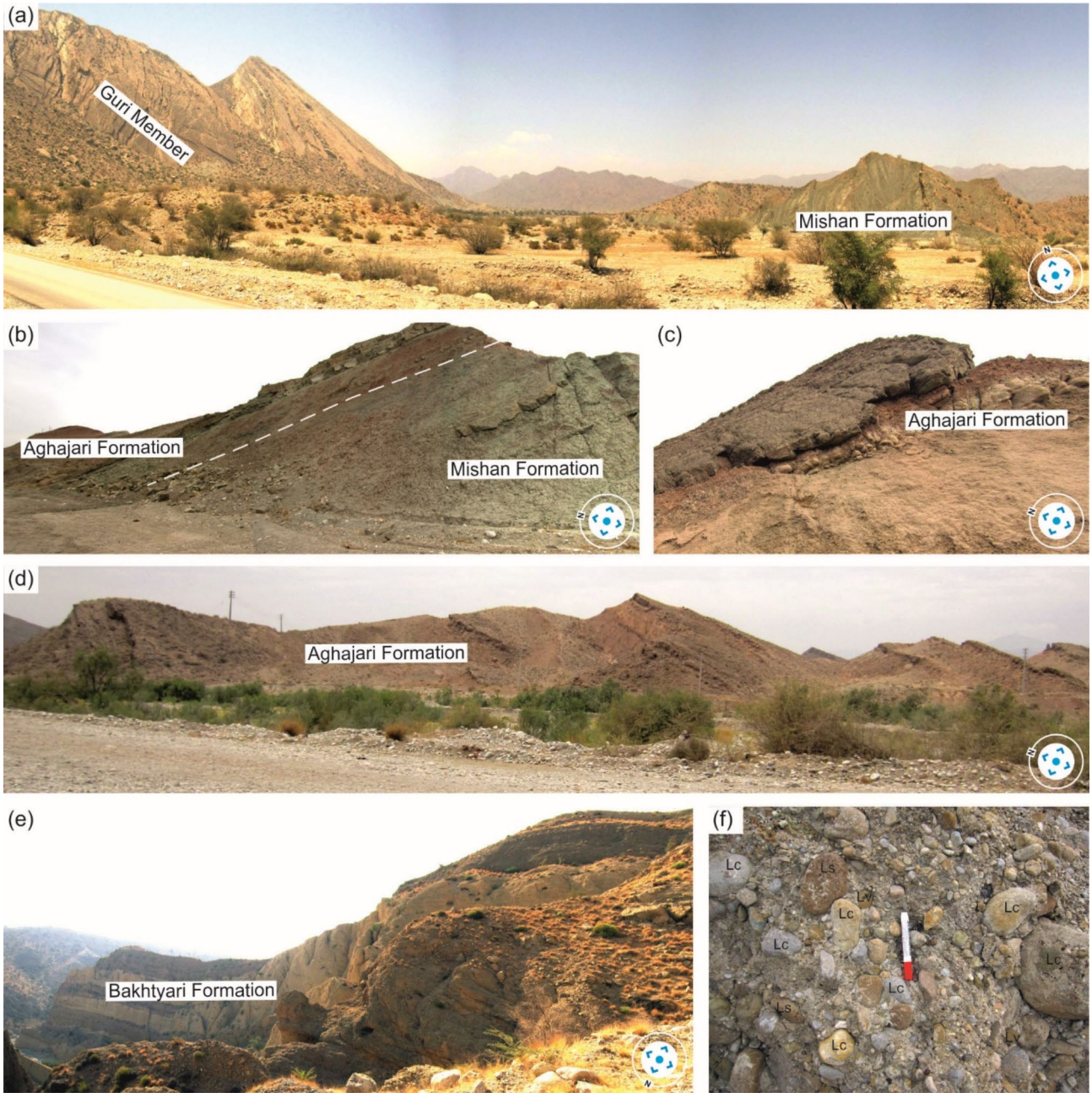

Fig. 5. Mio-Pliocene stratigraphy: (**a**) The Guri Limestone Member transitions up-section into marl and marly limestone of the Mishan Fm. in the Shamil area. (**b**) The green marls of Mishan Fm. passing up-section to red mudrock and sandstone of Aghajari Fm. in the Haji Abad area. (**c**) Channelized conglomerate embedded in red floodplain mudrock in the Aghajari Fm., Haji Abad area. (**d**) Alternating red mudrock, fluvial sandstone, and conglomerate in the Aghajari Fm., Haji Abad area. (**e**) Massive to thick-bedded conglomerates in the Bakhtyari Fm., Shamil area. (**f**) Dominant limestone pebbles in the Bakhtyari conglomerate. Abbreviations as in Fig. 6.

Sandstone petrography and U-Pb zircon ages

Upper Cretaceous Gurpi Formation The studied fine to coarse and poorly-sorted sandstones are litho-quartzose. Most quartz grains display straight extinction and embayments. The lithic grains are predominantly derived from felsic volcanic rocks, including rhyolite, rhyolitic tuff, metarhyolite, with minor chert, and limestone (Fig. 6a). Both plagioclase and K-feldspar exhibit only slight weathering. Most zircons yielded ages older than the Mesozoic, with a major peak at ~520 Ma (Cambrian) and a cluster around 793 Ma (Fig. 7b).

Upper *Oligocene-Lower Miocene Razak Formation* In the Haji Abad area, the red quartzo-lithic sandstones primarily consist of serpentinite[104], with subordinate amounts of radiolarite and carbonate grains (Fig. 6b). Conversely, in the Shamil area, litho-quartzose sandstones contain carbonate grains (limestone, silty limestone,

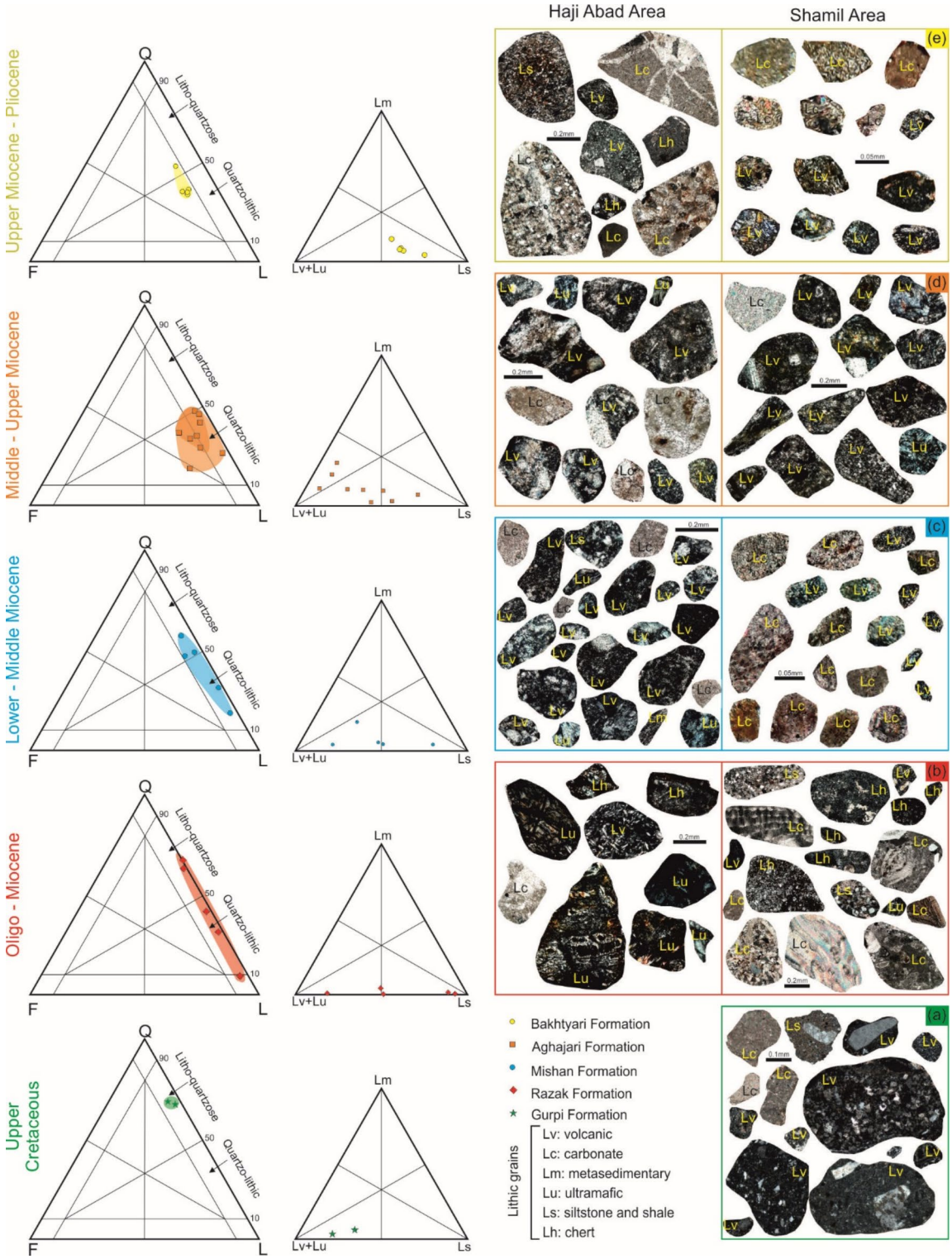

Fig. 6. Sandstone petrography (compositional fields after[93,94]): (**a**) Upper Cretaceous Gurpi Fm. (**b**) Upper Oligocene-Lower Miocene Razak Fm. (**c**) Lower-Middle Miocene Mishan Fm. (**d**) Middle-upper Miocene Aghajari Fm. (**e**) Upper Miocene-Pliocene Bakhtyari Fm.

marl), broken nummulites, and chert (Fig. 6b). Authigenic minerals include calcite, dolomite, gypsum, and iron oxides.

At the base of the Haji Abad section and in the Shamil area, zircon ages cluster at ~545 Ma, with a subordinate cluster at ~707 Ma (Fig. 7b). The youngest grain is dated at 87 + 3/-7 Ma (2σ), significantly older than the

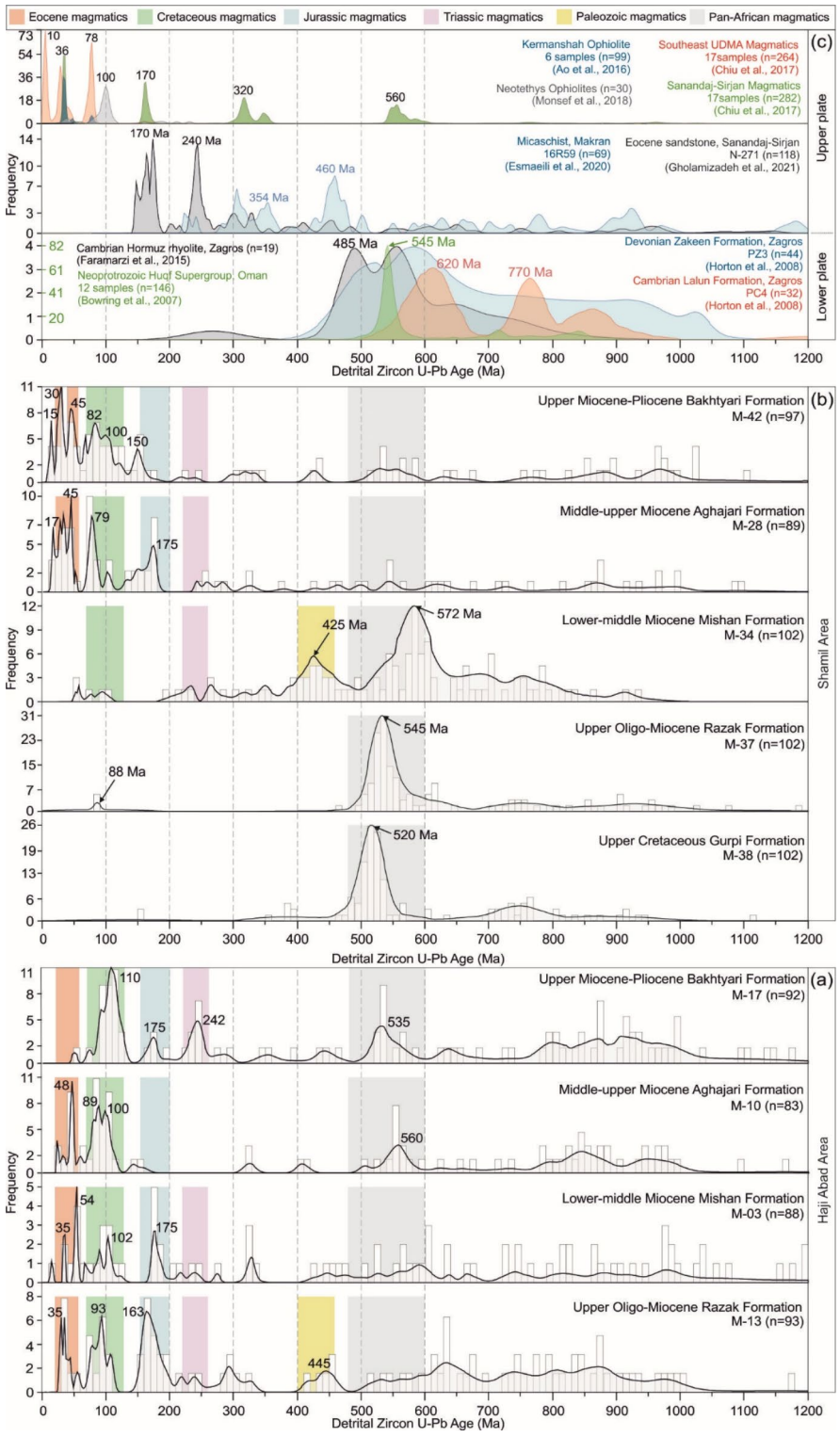

Fig. 7. The U-Pb age spectra of detrital zircon from the eastern Zagros Fold-Thrust Belt: (**a**) Haji Abad area. (**b**) Shamil area; (**c**) data compiled from previous studies.

depositional age. Samples collected up-section in the Haji Abad area display additional clusters around 10 Ma, 35 Ma, 93 Ma, 163 Ma, and 445 Ma (Fig. 7a), with the youngest grain dated at 31.3 + 0.7/-0.7 Ma (2σ).

Lower-Middle Miocene Mishan Formation The studied quartzo-lithic to litho-quartzose sandstones are moderately well-sorted. These sandstones are coarser in the Haji Abad area compared to those in the Shamil area (Fig. 6c). Volcanic and carbonate rock fragments, more prevalent in the Shamil area, are associated with slate,

schist, and metasedimentary lithic grains. Muscovite and biotite are also found in greater abundance in the Shamil area.

In the Haji Abad section, zircon ages cluster around 44 Ma, 99 Ma, 189 Ma, 570 Ma and 852 Ma (Fig. 7a), with the youngest grain dated at 17 + 2/-2 Ma (2σ). In contrast, zircon ages in the Shamil area cluster around 430 Ma, 572 Ma, and 754 Ma (Fig. 7b), with the youngest grain dated at 54 + 3/- Ma (2σ).

Middle-Upper Miocene Aghajari Formation The studied quartzo-lithic to feldspatho-quartzo-lithic sandstones mostly contain carbonate and volcanic lithic grains. The altered mafic to intermediate volcanic lithics, metamorphic lithics, feldspars, epidote, and tremolite are more prevalent in the Shamil area compared to the Haji Abad area (Fig. 6d). In contrast, carbonate and quartz grains are more abundant in the Haji Abad area, particularly at the top of the unit. Zircon ages cluster around 48 Ma, 89 Ma, 100 Ma, and 560 Ma in the Haji Abad section (Fig. 7a) and around 17 Ma, 45 Ma, 79 Ma, and 175 Ma in the Shamil area (Fig. 7b).

Upper Miocene-Pliocene Bakhtyari Formation The studied feldspatho-quartzo-lithic sandstones consist of sub-angular to sub-rounded chert, carbonate, sandy limestone, and minor microlithic volcanic lithic grains (Fig. 6e). These sandstones are coarser and richer in limestone lithics in the Haji Abad area. Zircon ages cluster around 110 Ma, 175 Ma, 242 Ma, and 535 Ma in the Haji Abad section, and around 15 Ma, 30 Ma, 45 Ma, 82 Ma, 100 Ma, and 150 Ma in the Shamil area (Fig. 7).

Trace elements and hafnium isotopes in detrital zircon

The trace element distribution in detrital zircon primarily falls within the continental-arc field of the Log_{10}(Nb/Yb)-Log_{10}(U/Yb) diagram[105] for all age groups (Fig. 8; Supplementary Table S4). Only five grains of disparate ages plot in the depleted mantle field, and a few Cretaceous zircons suggest a connection to MORB-type magmatism (Fig. 8).

Hafnium values (Hf) of zircon grains older than 400 Ma show a wide range from + 11 to -10 (Fig. 8e), whereas zircons younger than 200 Ma display more positive values ranging from + 15 to -3 (Fig. 8e; Supplementary Table S5).

Provenance analysis

Cenozoic strata in the Haji Abad area

The Upper Cretaceous-Paleocene Sachun Formation in the Haji Abad area documents a shallow-marine evaporitic environment with minor silisiclastic detritus. The oldest strata containing detritus likely originated from the Eurasia upper plate in the upper Oligocene-Lower Miocene Razak Formation. The composition of Oligo-Miocene to Pliocene sandstones reveals three major groups of source rocks (Fig. 6): (1) serpentinite and radiolarite from an ophiolite complex; (2) Cretaceous to Oligocene platform carbonates; (3) volcanic rocks ranging from basalt to rhyolite. Sedimentary and volcanic detritus increases at the expense of ophiolitic detritus in the overlying Mishan and Bakhtyari formations, carbonate detritus becoming dominant at the top of the succession (Fig. 6). The U-Pb age spectra of detrital zircon remain relatively consistent from the Upper Oligocene to Pliocene strata, reflecting Pan-African to Eocene magmatic events (Fig. 7) as will describe as follows:

Zircons aged at 44 – 35 Ma, with positive ε_{Hf} values, indicate a source from the igneous rocks of the Urumieh-Dokhtar Magmatic Arc[51] (Figs. 7 and 8). Zircon grains dated 78 – 67 Ma, with ε_{Hf} from + 5 to + 15, likely originated from the Sanandaj-Sirjan or southeastern Urumieh-Dokhtar Arc sources[51] (Fig. 8). A few zircons with 110 – 100 Ma age and ε_{Hf} between – 2 and + 3 (Fig. 8) suggest a provenance linked to continental magmatic rocks in the Sanandaj-Sirjan Zone[80] (Fig. 8). Reported values for zircons in the Neyriz ophiolite[5,24,76] (100 – 93 Ma, ε_{Hf} from + 10 to + 20) are underrepresented in our findings (Fig. 8), whereas zircons dated at 92 – 87 Ma point to provenance from the Sheikh Ali and DehSheikh ophiolites exposed to the northeast of the Main Zagros Thrust[57,85]. Jurassic zircons with 163 – 145 Ma ages and ε_{Hf} values from + 7 to + 10 correlate with those found in the Upper Jurassic ophiolite-bearing Bajgan Complex[58] (Figs. 2, 7a and 8) or in the Haji Abad-Esfandagheh ophiolitic belt. Furthermore, Jurassic zircons aged 182 – 175 Ma with ε_{Hf} values from – 5 to + 5 (Fig. 8), suggest contamination of mantle-derived magma with crustal materials in a continental-arc setting, particularly within the Sanandaj-Sirjan Zone in the Haji Abad area[5,51,57,80] (Figs. 2 and 7c). A few Triassic zircons aged at 240 Ma and ε_{Hf} values from – 5 to + 5, may be associated with igneous rocks formed during rifting of northeastern Gondwana,[106–107] which are exposed in the Surmaq and Eqlid areas of the Sanandaj-Sirjan Zone. Finally, zircons dated at 560 – 540 Ma appear to have been largely recycled from Paleozoic or Mesozoic strata rather than being directly sourced from the sparsely exposed Ediacaran-Cambrian basement in the Sanandaj-Sirjan Zone[52]. They may also have originated from Arabia basement rocks entrained in salt domes, particularly at the base of the Upper Oligocene-Lower Miocene Razak Formation[108]. Overall, these zircon age patterns suggest that detritus in the Upper Oligocene-Lower Miocene Razak Formation was chiefly supplied by the Eurasia upper plate.

Upper Cretaceous-Cenozoic strata in the Shamil area

Provenance of detritus in the Shamil area (Figs. 6 and 7) presents a distinct contrast to other areas, where the Upper Cretaceous sandstones are characterized by an abundance of felsic volcanic and recrystallized carbonate rock fragments, while ophiolitic detritus is notably absent.

U-Pb age-spectra of detrital zircon reveal a unimodal Ediacaran-Cambrian peak (545 – 520 Ma) in the Upper Cretaceous to Oligo-Miocene strata (Fig. 6). The zircon grains found in the conglomerate horizon intercalated with Upper Cretaceous pelagic limestones of the Gurpi Formation, are predominantly angular, indicating a first-cycle provenance rather than recycling. Ediacaran-Cambrian zircons characterize the Cambrian Lalun and Devonian Zakeen formations in the Zagros domain (Kuh-e Faraghan[109]) (Figs. 2 and 7c), as well as rhyolitic

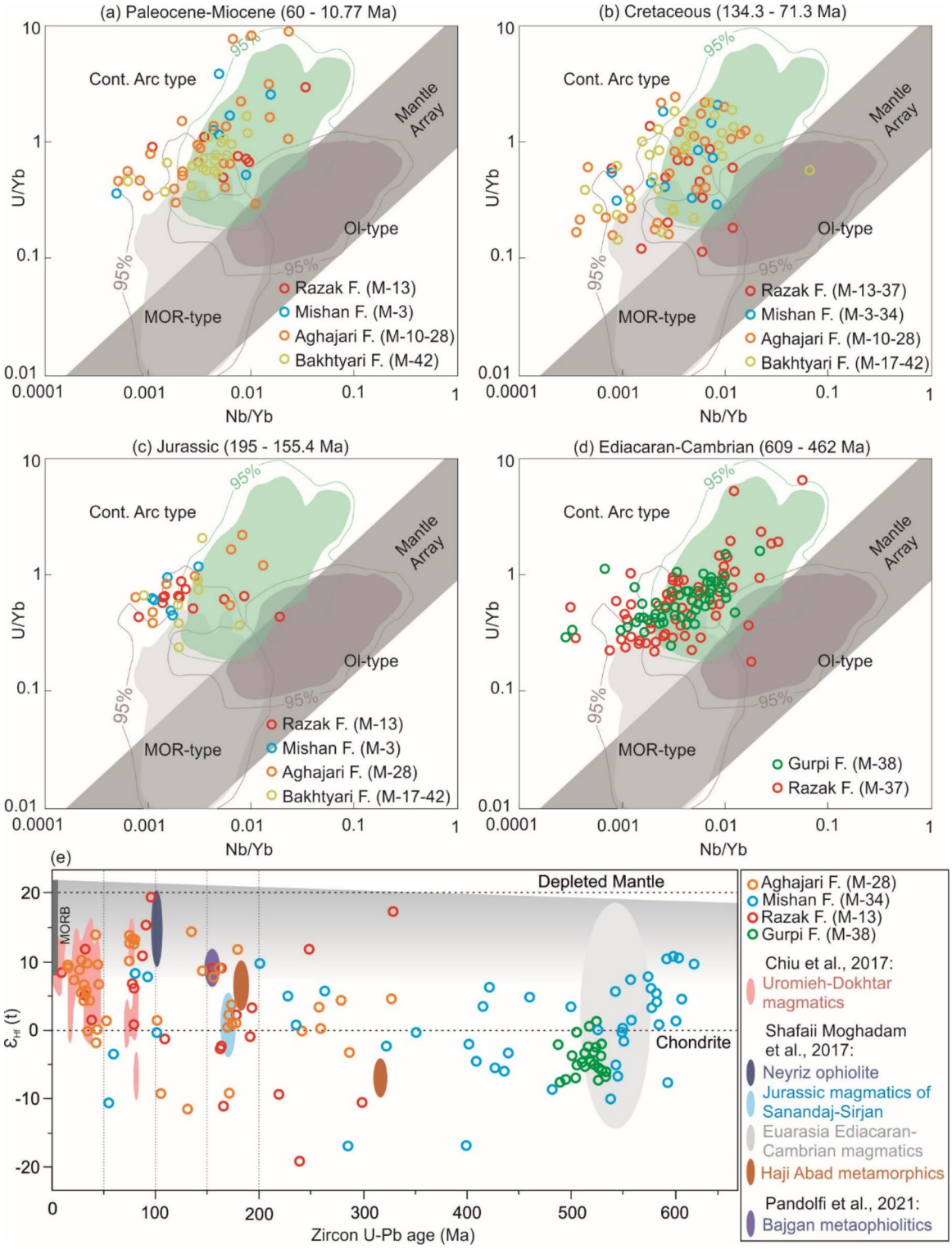

Fig. 8. (**a**-**d**) The trace element analysis of detrital zircon from Upper Cretaceous-Pliocene strata in the eastern Zagros Fold-Thrust Belt (Nb/Yb vs. U/Yb discrimination diagram after[105]). (**e**) The hafnium isotope signatures of these detrital zircons in eastern Zagros Fold-Thrust Belt. Depleted mantle field after[126].

rocks in the Cambrian Hormuz series (560 – 485 Ma[110]) (Fig. 7c) and Oman basement rocks[111]. Zircon grains dated at ~572 Ma (Ediacaran) and ~425 (Silurian) have been identified in the Lower-Middle Miocene Mishan Formation. These finding suggest that the Ediacaran zircons likely originated from Arabia, while the Silurian zircons may have come from metamorphosed Eurasia-margin rocks related to the rifting of Paleotethys[52,112].

The appearance of recycled Silurian zircons, associated with biotite and muscovite in the Lower-Middle Miocene Mishan Formation, marks the first evidence of detritus being shed from the Eurasia upper plate in this area.

The signature of Eurasia upper plate sources becomes dominant in the Middle-Upper Miocene Aghajari sandstones, including Cenozoic (54 – 15 Ma), Cretaceous (120 – 70 Ma), and Jurassic (170 – 150 Ma) zircon-age clusters (Fig. 7b). These zircons are inferred to have been derived from the Urumieh-Dokhtar Magmatic Arc[51], ophiolites and/or continental-arc and island-arc igneous rocks of the Sanandaj-Sirjan Zone, and magmatic rocks of the Sanandaj-Sirjan Zone, respectively[5,51] (Fig. 7c).

Exhumation of ophiolite complexes and other supra-subduction-zone rocks

Ultramafic and mafic rocks found in ophiolite complexes typically lack zircon, which is generally present only in specific igneous differentiates such as plagiogranites. However, by combining zircon ages, Cr-spinel frequency, and lithic grain assemblages, we can effectively trace the exhumation of ophiolite bodies and associated rocks through time and space. Two types of supra-subduction sources can be distinguished based on our data (Figs. 7 and 8):

1) obducted Neyriz and Samail ophiolites. Detrital zircons yielding ages 110 – 93 Ma with ε_{Hf} values from +7 to +20 found in Upper Cretaceous-Paleocene sandstones of the Neyriz area[5] (Fig. 7), may have originated from the Neyriz ophiolite (100 – 93 Ma[75–76]). In contrast, ophiolitic detritus is conspicuously absent in the Upper Cretaceous-Paleocene strata exposed in the Shamil area (Figs. 7 and 8);

(2) other supra-subduction-zone magmatic rocks. Detrital zircons yielding 92 – 87 Ma ages with ε_{Hf} values from +7 to +15 suggest a derivation from magmatic sources associated with ophiolite-bearing complexes found in the Haji Abad area, which is exposed close to the Main Zagros Thrust[85] (Figs. 2 and 8). For instance, Plagiogranites and dacites dated at 91 – 87 Ma, have been identified near the Dehsheikh ophiolitic complex[85] (Fig. 2). Additionally, older Late Jurassic zircons, dating at 160 – 145 Ma with ε_{Hf} values from +7 to +10, have been documented in both Haji Abad and Shamil areas (Figs. 7 and 8). These zircon ages correspond with the meta-ophiolitic bodies found in the Bajgan subduction complex (161 to 114 Ma[59]) (Fig. 2). A few detrital zircons dated at ~186 – 174 Ma, may have been originated from meta-intrusive rocks of the Haji Abad-Esfandagheh ophiolitic belt[57,84], which were accreted to the Eurasia margin and are exposed northeast of the Main Zagros Thrust. Jurassic-Cretaceous sedimentary and igneous rock cover, and underling by ophiolite bearing Eo-Oligocene turbidites, indicates that these ophiolitic rocks were formed or emplaced along the active margin of Eurasia[47,60].

The first evidence of ophiolitic detritus in the Zagros sedimentary succession is found in the form of serpentinite and Cr-spinel grains within the Maastrichtian-Paleocene Sachun Formation in the Neyriz area, as well as in the Upper Oligocene-Lower Miocene Razak Formation in both Haji Abad and Shamil areas (Fig. 6b). Zircon grains in the Razak Formation exhibit ε_{Hf} values of < 15, contrasting with ε_{Hf} values > 15 for Upper Cretaceous-Paleocene sediments[5] inferred to originate from the Neyriz ophiolite (Fig. 8-e). This distinction suggests that the ophiolite bodies exhumed during the Oligocene-Early Miocene were seemingly different in origin and setting compared to those exhumed earlier during the Late Cretaceous-Paleocene.

Cenozoic evolution of the eastern Zagros Fold-Thrust Belt

The Haji Abad and Shamil areas in the eastern Zagros Fold-Thrust Belt recorded different responses to Cretaceous ophiolite emplacement and tectonic events. The Haji Abad area has been affected by the Main Zagros Thrust to the northeast, whereas the Shamil area mainly reflected tectonic stresses related to Oman during the Paleogene, and Minab-Zendan Fault activity during the Neogene (Figs. 9 and 10).

Late Cretaceous-Early Paleocene Detrital zircons yielding 110 – 93 Ma ages with ε_{Hf} values from +7 to +20 in the Upper Cretaceous-Paleocene Sachun Formation exposed in the Neyriz area[5] (Fig. 7) may have been derived from the Neyriz ophiolite (100 – 93 Ma[75–76]). The Sachun Formation, ~300 m-thick, was deposited in a shallow-marine environment and contains ophiolitic detritus[66]. In the Haji Abad area –far away from Neyriz– this formation with only ~80 m-thick lacks interbedded siliciclastic detritus, indicating a transition to an evaporitic marginal sea (Figs. 3 and 10a). The coeval deep-marine Gurpi Formation, ~1500 m-thick in the Shamil area[67], predominantly yields Ediacaran-Early Cambrian zircon ages clustering around 520 Ma. These zircons may have originated from xenoliths within the Hormuz salt, exposed at the surface along major faults during a time of high convergence rates (~2 cm/year[47]). A thrust-fault system similar as the major Hagab thrust to the west of Musandam may have been active to the east of the Shamil area at that time (Fig. 10a).

Late Paleocene-Middle Eocene No clastic detritus was supplied to the Arabia plate at this time. The top of the Jahrum Formation near the Shamil area dated as Bartonian[113] (Late Eocene), becomes shallower and older (middle Eocene, Lutetian) toward the northwest (Neyriz area). The unconformity at the top of the Jahrum Formation (Fig. 3) may have formed during a marine regression associated with the closure of the Neotethys Ocean[36]. However, a narrow seaway remained open between the Arabia and Eurasia continental masses during this time (Fig. 10b).

Oligocene-Early Miocene The upper Oligocene-Lower Miocene Razak Formation contains two distinct groups of detrital components: quartz, carbonate, chert, siltstone, and felsic volcanic lithic grains originated most probably from the Hormuz rhyolitic series (520–540 Ma: Figures 6 and 7, and 9), whereas serpentinite, radiolarite, carbonate, and mafic to intermediate volcanic lithic grains were shed from ophiolitic sequences and Jurassic-Eocene volcanic rocks of the Eurasia upper plate (35, 92, 172 Ma: Figures 6, 7 and 9). The first group of detrital components, of Arabia lower plate provenance is primarily found at the base of the Razak Formation in the Neyriz and Haji Abad areas and throughout the unit in the Shamil area. The second group of components is dominant

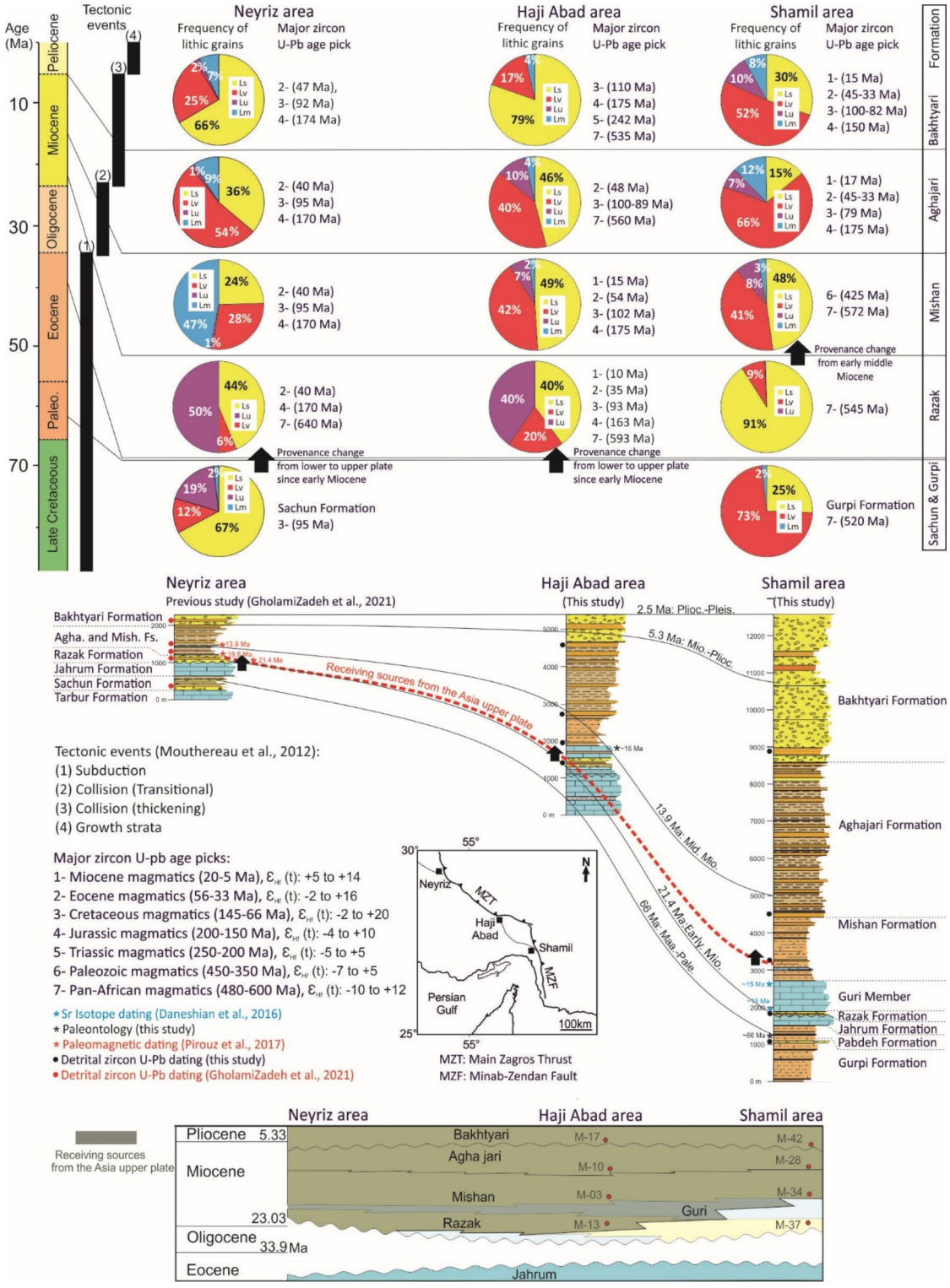

Fig. 9. Integration of stratigraphic, petrographic, and detrital zircon ages from the eastern Zagros Fold-Thrust Belt (see Fig. 3 for regional distribution of rock units). Lithofacies become progressively younger and thicker from northwest to southeast along the Zagros Suture Zone. Sandstone petrography and zircon ages highlight changes in provenance both up-section and along the Main Zagros Thrust.

in most of the Razak Formation exposed in the Neyriz and Haji Abad areas. The regional differences in provenance may be attributed to a variety of factors, including age, exposed lithologies, erosion and subsidence rates, paleo-drainage systems, and the irregular shape of the Arabia margin (Figs. 3 and 9). The higher erosion rate at the base of Razak Formation in the Neyriz compared to Shamil suggest more intense erosion on paleo-highs

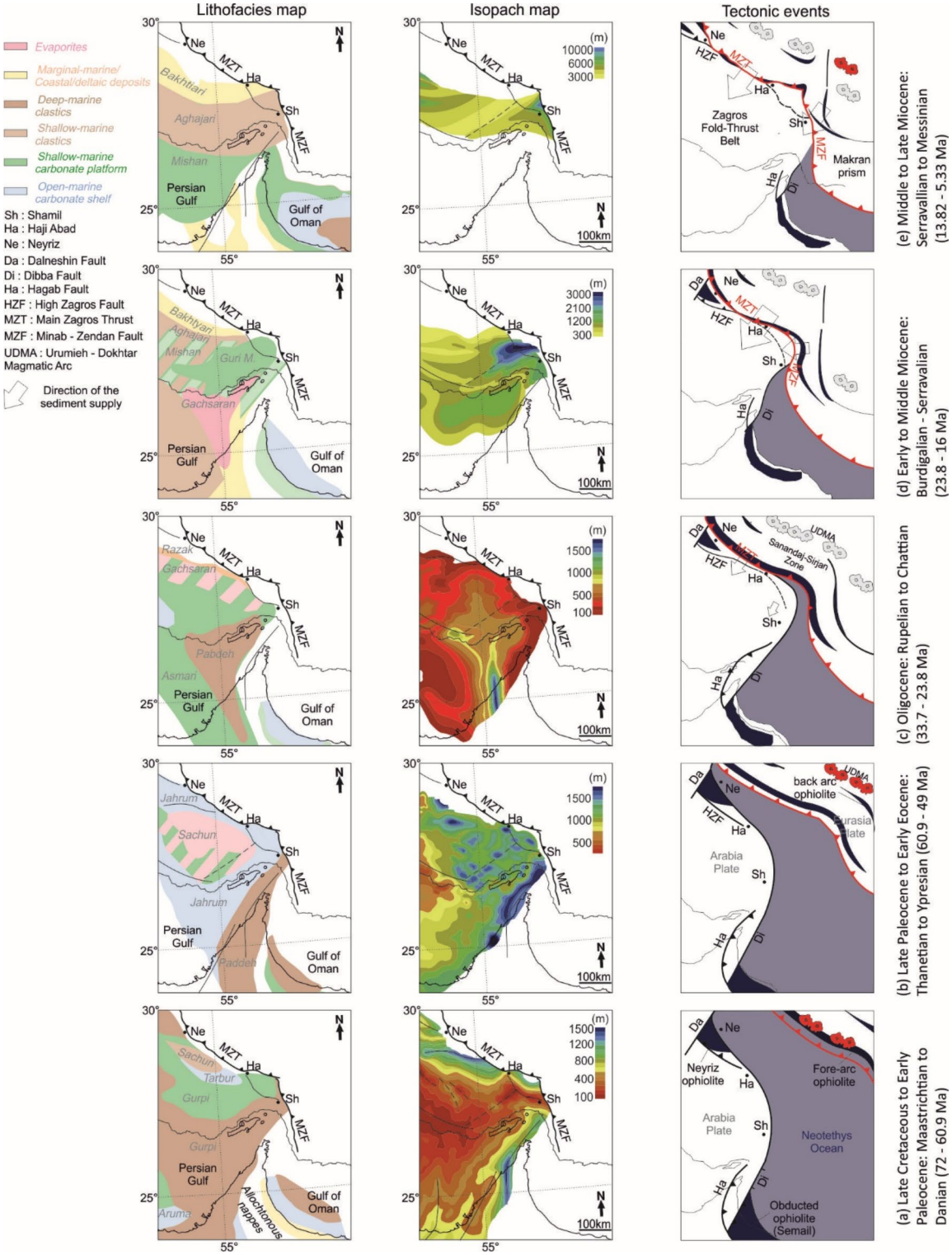

Fig. 10. Paleogeographic and tectonic reconstructions of Upper Cretaceous-Cenozoic Zagros Fold-Thrust Belt (lithofacies and isopach maps modified from Motiei[69]). See text for full explanation.

associated with obducted terranes (Figs. 3, 9 and 10c). The initial subduction of the Arabia continental margin beneath the Sanandaj-Sirjan Zone[38,114] (Fig. 10c) led to strong compressive stresses. This led to the emplacement and exhumation of supra-subduction-zone ophiolites and magmatic rocks during the Late Eocene-Oligocene[13] (Fig. 10c), and uplift of the Arabia and Eurasia margins along the Main Zagros Thrust[13,54,115]. At this time, the Neotethys seaway still remained partially open to the west of the Shamil area and Minab-Zendan Fault, which is linked to the Main Zagros Thrust[41] (Fig. 10c).

Early- middle Miocene Both Neyriz and Haji Abad areas, along the Main Zagros Thrust, continued to receive detrital zircons dated at ~ 15 Ma, 54 – 40 Ma, 102 – 90 Ma, and 175 – 170 from the Eurasia upper plate during this time (Fig. 9). However, the Shamil area not only received detritus from the Eurasia upper plate for the first time but also exhibited different sources compared to Neyriz and Haji Abad. It has received mostly zircons dated as ~ 572 Ma from the Arabia basement, plus Silurian zircons with ages clustering around 425 Ma that were recycled from older metamorphosed siltstone and sandstones (Figs. 7, 9 and 10d). The differing signatures from the Eurasia upper plate in the Haji Abad and Shamil areas may reflect different distribution of source-rock lithologies, different paleo-dispersal patterns, activity along the Minab-Zendan fault system, or diachronous collisional processes. At this time, sedimentary facies and stratal thickness display a distinct change due to Minab-Zendan Fault activity since the Burdigalian (Early Miocene) (Figs. 9 and 10d), when this area was characterized by deeper marine environments documented by pelagic foraminifera[116]. This abrupt transition is likely attributable to the flexural response of the Arabia plate to loading of the ophiolite and Makran accretionary prism to the east of the Minab-Zendan Fault[115,117]. At this time, both the collided Arabia and Eurasia margins experienced uplift to the east of Shamil.

Middle Miocene-Pliocene Detrital zircons from Miocene (~ 17 Ma), Eocene (~ 45 – 33 Ma), Cretaceous (~ 79 Ma), and Jurassic (~ 135 Ma) igneous rocks of the Eurasia upper plate continued to be deposited in the Aghajari Formation extended from the Neyriz and Haji Abad areas to the Shamil area (Figs. 7, 9 and 10e). In the Shamil area, the appearance a younger cluster of detrital zircons dated as ~ 17 – 15 Ma reflects the erosion of the younger part of the southeastern Urumieh-Dokhtar Magmatic Arc[16,51]. (Figures 7 and 9). The base of the Aghajari Formation has been magnetostratigraphically dated at 13.9 Ma in Neyriz[23] and biostratigraphically identified as Serravalian in the Shamil area[103,116,118]. The combined thickness of the Aghajari and Bakhtyari formations increases up to ~ 10,000 m indicating ongoing activity of the Minab-Zendan Fault (Fig. 10e).

Collision timing in the eastern Zagros Fold-Thrust Belt

The onset of continental subduction was initially characterized by erosional exhumation and crustal shortening in the lower and upper plates[29]. This shortening facilitated the formation of a flexural fore-bulge and an erosional unconformity on the passive margin. As continental collision progressed, the orogenic wedge between the two plates was uplifted, leading to sediment shedding into the lower plate foreland basin. The first arrival of detritus from the upper plate to the lower plate provides a robust minimum age for oceanic closure, the onset of continental subduction, and the formation of a syn-collisional foreland basin, as indicated by provenance studies[2,8,119]. Thus, the time span from the age of the erosional surface to the oldest depositional age of receiving detritus from the upper plate reflects a progressive collision.

In the eastern Zagros Fold-Thrust Belt, the regional unconformity at the top of the Jahrum Formation likely represents erosion associated with fore-bulge development[23,53,68–69] (Fig. 3). The age of the top of the Jahrum Formation varies from the Middle Eocene in the northwest (Neyriz region) to the Late Eocene to the southeast (Shamil area) (Fig. 3). The Middle-Late Eocene period aligns with the initial shortening and collision timing recorded in the Eurasia upper plate[13,114].

Changes of zircon-age spectra in space and time provide further evidence (Fig. 9). At the base of the Razak Formation, exposed in the Neyriz and Haji Abad areas, detrital zircons dated at 540–560 Ma, indicative of Arabia provenance, are predominant. They are replaced up-section by zircons with ages clustering around 175 – 163 Ma, 110 – 88 Ma, 54 – 35 Ma, 17 – 5 Ma, all derived from the Eurasia upper plate[120] (Figs. 7 and 9). Instead, detrital zircons yielding latest Neoproterozoic ages (~ 545 Ma) remain dominant in the Shamil area. Not only provenance but also strata thickness and depositional environments changed within the Razak Formation (Fig. 10c), from chiefly braided river and fan delta in the Neyriz and Haji Abad areas to costal-evaporitic and marginal sea setting in the Shamil area, resulting in a much thinner unit (~50 m vs. ~200 m) (Figs. 9 and 10). The base of the Razak Formation is dated at 21.4 Ma in the Neyriz area[23], while the underlying unconformity capping the Eocene Jahrum Formation corresponds to a more extended time gap in the Neyriz and Shamil areas compared to Haji Abad (Fig. 3). This 'provenance revolution' is particularly evident in the Upper Oligocene/Lower Miocene Razak Formation exposed in the Neyriz area to the northwest of the Haji Abad area close to the Main Zagros Thrust, and in the lower Langhian strata of the Mishan Formation in the Shamil area to the east of the Minab-Zendan Fault (Fig. 9). The predominant Pan-African zircon sources in the Shamil area during the Late Oligocene-Early Miocene may be attributed to the elevated and buoyant eastern Arabia margin, which facilitated the transport of orogenic deposits through an axial drainage system along the Main Zagros Thrust into the trench basin between the Zagros and Makran domains.

The Langhian Mishan Formation reaches a maximum thickness of ~2500 m near the Minab-Zendan Fault, suggesting significant fault activity during this time (Fig. 10d). The Middle Miocene unconformity, well-documented by seismic surveys across the Persian Gulf and Strait of Hormuz[102,121–122], as well as west of the Musandam Peninsula[123], truncates underlying Cretaceous to lower Miocene sedimentary units, including the Burdigalian Guri Member[102]. Recent study has suggested that this unconformity may be older (Early Miocene) in these regions and is overlain by the Guri Member of Mishan Formation[68].

Consequently, the onset of continent-continent collision is constrained to pre-Late Oligocene in Neyriz and Haji Abad areas and pre-Middle Miocene in the Shamil area. Provenance changes through time and space in the eastern Zagros Fold-Thrust Belt, when integrated with facies changes and isopach maps reveal the regional differences in the geological history, source area evolution, and paleo-dispersal patterns.

Conclusions

The stratigraphic, sedimentological, and provenance analysis of Upper Cretaceous to Pliocene strata exposed in the eastern Zagros Fold-Thrust Belt led to the following key findings:

- The obduction of Cretaceous ophiolite onto the northeastern margin of Arabia was not a uniform process; rather, it occurred through the movement of individual thrust sheets. The Haji Abad and Shamil areas did not receive detritus from these obducted ophiolites during the Late Cretaceous.
- In the latest Cretaceous, the exhumation of the Arabia Pan-African basement occurred within deep-marine environments of the Arabia continental shelf. This process was driven by fault-induced salt-dome diapirism, as evidenced by ~520-Ma-old zircons in the Gurpi Formation.
- The sandstones of the Razak Formation reveal changes in provenance and depositional facies over time and space. The base of the Razak Formation in the Neyriz, Haji Abad, and Shamil areas received detritus only from Arabia, indicated by a dominance of late Neoproterozoic zircons (540 Ma and older).
- In the Haji Abad area, detritus from the Eurasia upper plate was first documented in the upper part of the Razak Formation, as shown by abundant zircon grains with ages raging from Miocene (15 – 10 Ma) to Eocene (54 – 35 Ma), Cretaceous (110 – 89 Ma), and Jurassic (175 – 163 Ma). Zircons dated at 91 – 87 Ma, 160 – 145 Ma, and 161 – 114 Ma suggest a provenance linked to magmatic arcs and ophiolite complexes.
- In contrast, the Shamil area along the Minab-Zendan Fault did not recorded any detritus from the Eurasia upper plate until the deposition of the early Middle Miocene (Langhian) Mishan Formation, which here unconformably overlies Cretaceous to Lower Miocene strata and reaches maximum thickness.
- Our findings reveal that the Arabia- Eurasia collision was already underway by the Late Oligocene in the northwestern regions (Neyriz and Haji Abad areas along the Main Zagros Thrust) and became more pronounced by the Middle Miocene (Langhian) in the southeastern (Shamil area along the Minab-Zendan Fault).
- Lateral variations in sediment composition may reflect not only heterochrony in the geology of the source area but also variations in the collisional process, changes in paleo-dispersal patterns and a progressive eastward shift through time.

Our results advocate for more detailed investigations into ophiolite emplacement along the Main Zagros Thrust, as well as integrated studies of stratigraphy, structural geology, and provenance on a broader scale.

Data availability

Location of samples for zircon analyses and the datasets generated during this study are provided in Supplementary Table S1-5. Point-counting results plotted on diagrams in Fig. 6 are provided in Supplementary Table S2, U-Pb and REE data on detrital zircon can be found in Supplementary Tables S3 and S4, while Hf isotopic data are available in Supplementary Table S5. Further inquiries, please contact the corresponding author.

Received: 31 May 2024; Accepted: 11 February 2025
Published online: 19 February 2025

References

1. Garzanti, E., Doglioni, C., Vezzoli, G. & Andò, S. Orogenic belts and orogenic sediment provenance. *J. Geol. v*. **115**, 315–334 (2007).
2. Hu, X. et al. The timing of India-Asia collision onset—Facts, theories, controversies: Earth-Science Reviews, v. 160, pp. 264–299, (2016). https://doi.org/10.1016/j.earscirev.2016.07.014
3. Hu, X., JianGang, W., Wei, A., Garzanti, E. & Juan, L. Constraining the timing of the India-Asia continental collision by the sedimentary record. *Sci. China Earth Sci. v*. **60**, 603–625. https://doi.org/10.1007/s11430-016-9003-6 (2017).
4. GholamiZadeh, P. et al. Revised version of the cenozoic collision along the Zagros Orogen, insights from Cr spinel and modal analyses: scientific reports, v. 7, 10828, pp. 1–7, (2017). https://doi.org/10.1038/s41598-01711042-1
5. GholamiZadeh, P., Hu, X. M., Garzanti, E. & Adabi, M. H. Constraining the timing of Arabia-Eurasia collision in the Zagros orogen by sandstone provenance (Neyriz, Iran): Geological Society of America Bulletin, v. 134, pp. 1793–1810, (2022). https://doi.org/10.1130/B35950.1
6. Critelli, S. Provenance of mesozoic to Cenozoic Circum-Mediterranean sandstones in relation to tectonic setting. *Earth Sci. Rev.* **185**, 624–648. https://doi.org/10.1016/j.earscirev.2018.07.001 (2018).
7. Critelli, S. & Criniti, S. Sandstone Petrology and Provenance in Fold Thrust Belt and Foreland Basin System, *in* Ali Ismail Al-Juboury, ed., Sedimentary Petrology - Implications in Petroleum Industry: Intech Open Access Publisher, Janeza Trdine 9, Rijeka, Croatia, pp. 1–15, (2021). https://doi.org/10.5772/intechopen.96985
8. Garzanti, E., Baud, A. & Mascle, G. Sedimentary record of the northward flight of India and its collision with Eurasia (Ladakh Himalaya, India). *Geodinamica Acta v*. **1** (4–5), 297–312 (1987).
9. Zhang, Z. Y. et al. Detrital zircon provenance analysis in the Zagros Orogen, SW Iran: implications for the amalgamation history of the neo-tethys: International Journalof Earth Sciences, v. 106, pp. 1223–1238, (2017). https://doi.org/10.1007/s00531-016-1314-3
10. Koshnaw, R. I., Stockli, D. F. & Schlunegger, F. Timing of the Arabia-Eurasia continental collision—evidence from detrital zircon U-Pb geochronology of the Red Bed Series strata of the northwest Zagros Hinterland, Kurdistan region of Iraq. *Geology*, v. 47, pp. 47–50. (2018).
11. Barber, D. E., Stockli, D. F. & Galster, F. The Proto-Zagros foreland basin in Lorestan, western Iran—insights from multi-mineral detrital geo-thermochronometric and trace-elemental provenance analysis: Geochemistry, Geophysics, Geosystems, v. 20, pp. 2657–2680, (2019). https://doi.org/10.1029/2019GC008185
12. Wu, F., Wan, B., Zhao, L., Xiao, W. & Zhu, R. Tethyan geodynamics: Acta Petrol. Sinica, 36, 1627–1674. (2020).
13. Agard, P. et al. Zagros orogeny: A subduction-dominated process: Geological Magazine, v. 148, pp. 692–725, (2011). https://doi.org/10.1017/S001675681100046X
14. McQuarrie, N. & van Hinsbergen, D. J. J. Retrodeforming the Arabia-Eurasia collision zone: age of collision versus magnitude of continental subduction. *Geol. v*. **41**, 315–318 (2013).
15. Verdel, C., Wernicke, B. P., Hassanzadeh, J. & Guest, B. A paleogene extensional arc flare-up in Iran. *Tectonics* **v. 30** https://doi.org/10.1029/2010TC002809 (2011).

16. Chiu, H. Y. et al. Zircon U–Pb age constraints from Iran on the magmatic evolution related to Neotethyan subduction and Zagros orogeny. *Lithos* **v. 162–163**, p70–87. https://doi.org/10.1016/j.lithos.2013.01.006 (2013).
17. Zhang, Z. Y. et al. Geochemistry, zircon U-Pb and hf isotope for granitoids, NW Sanandaj-Sirjan zone, Iran: implications for mesozoic-cenozoic episodic magmatism during neo-tethyan lithospheric subduction: Gondwana Research, v. 62, pp. 227–245, (2018). https://doi.org/10.1016/j.gr.2018.04.002
18. Moghadam, H. S. et al. The middle–late cretaceous Zagros ophiolites, Iran: linking of a 3000 km swath of subduction initiation fore-arc lithosphere from Troodos, Cyprus to Oman. Bulletin, v.134, pp. 1414–1442, (2022). https://doi.org/10.1130/B36041.1
19. Alavi, M. Tectonics of the Zagros orogenic belt of Iran: New data and interpretations: Tectonophysics, v. 229, pp. 211–238, (1994). https://doi.org/10.1016/0040- 1951(94)90030-2.
20. Fakhari, M. D., Axen, G. J., Horton, B. K., Hassanzadeh, J. & Amini, A. Revised age of proximal deposits in the Zagros foreland basin and implications for cenozoic evolution of the high Zagros: tectonophysics, v. 451, pp. 170–185, (2008). https://doi.org/10.1016/j.tecto.2007.11.064
21. Homke, S. et al. Insights in the exhumation history of the NW Zagros from bedrock and detrital apatite fission-track analysis: evidence for a long-lived orogeny. *Basin Res. v*. **22** (5), 659–680. https://doi.org/10.1111/j.1365-2117.2009.00431.x (2010).
22. Khadivi, S., Mouthereau, F., Barbarand, J., Adatte, T. & Lacombe, O. Constraints on paleodrainage evolution induced by uplift and exhumation on the southern flank of the Zagros–Iranian Plateau. *J. Geol. Soc. v*. **169**, 83–97. https://doi.org/10.1144/0016-76492011-031 (2012).
23. Pirouz, M., Avouac, J. P., Hassanzadeh, J., Kirschvink, J. L. & Bahroudi, A. Early neogene foreland of the Zagros, implications for the initial closure of the neo- Tethys and kinematics of crustal shortening. *Earth Planet. Sci. Lett.* **v. 477**, p168–182. https://doi.org/10.1016/j.epsl.2017.07.046 (2017).
24. Cai, F. L. et al. Configuration and timing of collision between Arabia and Eurasia in the Zagros collision zone, Fars, southern Iran. *Tectonics v*. 40. https://doi.org/10.1029/2021TC006762 (2021).
25. Sun, G. et al. Pre-eocene Arabia-Eurasia collision: new constraints from the Zagros Mountains (Amiran Basin, Iran). *Geology* **v. 51**, p941–p946. https://doi.org/10.1130/G51321.1 (2023).
26. Okay, A. I., Zattin, M. & Cavazza, W. Apatite fission-track data for the Miocene Arabia-Eurasia collision: Geology, v. 38, pp. 35–38, (2010). https://doi.org/10.1130/G30234.1
27. Cavazza, W., Catto, S., Zattin, M., Okay, A. & Reiners, P. Thermochronology of the Miocene Arabia-Eurasia collision zone of southeastern Turkey: Geosphere, v. 14, 5, pp. 2277–2293, (2018). https://doi.org/10.1130/GES01637.1
28. Darin, M. H., Umhoefer, P. J. & Thomson, S. N. *Rapid late Eocene Exhumation of the Sivas Basin (Central Anatolia) Driven by Initial Arabia-Eurasia Collision*v.37p.3805–3833 (Tectonics, 2018). https://doi.org/10.1029/2017TC00495410
29. Darin, M. H. & Umhoefer, P. J. Diachronous initiation of Arabia–Eurasia collision from eastern Anatolia to the southeastern Zagros Mountains since middle Eocene time. *Int. Geol. Rev. v*. **64** (18), 2653–2681. https://doi.org/10.1080/00206814.2022.2048272 (2022).
30. Khadivi, S. et al. Magnetochronology of synorogenic miocene foreland sediments in the fars arc of the Zagros Folded Belt (SW Iran): Basin Research, v. 22, pp. 918–932, (2010). https://doi.org/10.1111/j.1365-2117.2009.00446.x
31. Jackson, J. A. Reactivation of basement faults and crustal shortening in orogenic belts: Nature, v. 283, p. 343 – **346**, (1980). https://doi.org/10.1038/283343a0
32. Berberian, M. Master blind thrust faults hidden under the Zagros folds: active basement tectonics and surface morphotectonics: tectonophysics, v. 241, pp. 193–224, (1995). https://doi.org/10.1016/0040-1951(94)00185-C
33. Angiolini, L., Balini, M., Garzanti, E., Nicora, A. & Tintori, A. Gondwanan deglaciation and opening of neotethys: the Al Khlata and Saiwan formations of Interior Oman: Palaeogeography, Palaeoclimatology. *Palaeoecology v*. **196** (1–2), 99–123 (2003).
34. Critelli, S. & Martín-Martín, M. History of western Tethys Ocean and the birth of the circum-Mediterranean orogeny as reflected by source-to-sink relations. *Int. Geol. Rev. v*. **66** (2), 505–515. https://doi.org/10.1080/00206814.2023.2280787 (2024).
35. Wan, B. et al. When and why the NeoTethyan Subduction Initiated along the eurasian margin: a Case Study from a jurassic Eclogite in Southern Iran. *Compressional Tectonics: Plate Convergence Mountain Building*. **v. 1**, 245–260 (2023).
36. Ricou, L. E. Le croissant ophiolitique péri-arabe, une ceinture de nappes mise en place Au crétacé supérieur. *Rev. Géogr. Phys. Géol. Dyn*. **v. 13**, 327–350 (1971).
37. Saura, E. et al. Basin architecture and growth folding of the NW Zagros early foreland basin during the late cretaceous and early Tertiary. *J. Geol. Soc. v*. **168**, 235–250. https://doi.org/10.1144/0016-76492010-092 (2011).
38. Mouthereau, F., Lacombe, O. & Verges, J. Building the Zagros collisional orogen: timing, strain distribution and the dynamics of Arabia/Eurasia plate convergence. *Tectonophysics* **v. 532**, p27–60. https://doi.org/10.1016/j.tecto.2012.01.022 (2012).
39. McCall, G. J. H. & Kidd, R. G. W. The Makran southeastern Iran: the anatomy of a convergent plate margin from cretaceous to Present, in Trench Forearc Gelogy, pp. 387–397. (1982). ed. Legget, J.K., Geol. Soc of London, Spec. Publ.
40. Critelli, S., De Rosa, R. & Platt, J. P. Sandstone detrital modes in the Makran accretionary wedge, southwest Pakistan: implications for tectonic setting and long-distance turbidite transportation. *Sed. Geol.* **68**, 241–260. https://doi.org/10.1016/0037-0738(90)90013-J (1990).
41. Regard, V. et al. The transition between Makran subduction and the Zagros collision: recent advances in its structure and active deformation. *Geol. Soc. Lond. Spec. Publ.* **330** (1), 43–64. https://doi.org/10.1144/SP330.4 (2010).
42. Paul, A., Hatzfeld, D., Kaviani, A., Tatar, M. & Péquegnat, C. Seismic imaging of the lithospheric structure of the Zagros mountain belt (Iran), in Tectonic and Stratigraphic Evolution of Zagros and Makran During the Mesozoic-Cenozoic, edited by P. Leturmy, and C. Robin, Geol. Soc. London, Spec. Publ., 330, pp. 5–18. (2010).
43. Alavi, M. Regional stratigraphy of the Zagros fold-thrust belt of Iran and its proforeland evolution. *Am. J. Sci. v*. **304**, 1–20. https://doi.org/10.2475/ajs.304.1.1 (2004).
44. Glennie, K. W. et al. Geology of the Oman Mountains. The Hague, Verhandelingen Van Het Koninklijk Nederlands Geologisch Mijnbouwkundig Genootschap. *Transactions* **31**, 423 (1974).
45. Searle, M. P. & Cox, J. S. Tectonic setting, origin and obduction of the Oman ophiolite. *Geol. Soc. Am. Bull.* **v. 111**, p104–p122 (1999).
46. Stöcklin, J. Structural history and tectonics of Iran: a review: AAPG (Am. Assoc. Pet. *Geol.) Bull. V*. **52**, 1229–1258 (1968).
47. Agard, P. et al. Transient, synobduction exhumation of Zagros blueschists inferred from P-T, deformation, time, and kinematic constraints: implications for neotethyan wedge dynamics. *J. Geophys. Res.* **111**, B11401. https://doi.org/10.1029/2005JB004103 (2006).
48. Verdel, C. et al. Geology and thermochronology of Tertiary Cordilleran-style metamorphic core complexes in the Saghand region of central Iran: Geol. *Soc. Am. Bull. v*. **119**, 961–977. https://doi.org/10.1130/B26102.1 (2007).
49. Mahmoudi, S., Corfu, F., Masoudi, F., Mehrabi, B. & Mohajjel, M. U-Pb dating and emplacement history of granitoid plutons in the northern Sanandaj-Sirjan Zone. *Iran: J. Asian Earth Sci. v*. **41** (3), 238–249. https://doi.org/10.1016/j.jseaes.2011.03.006 (2011).
50. Mohajjel, M., Fergusson, C. I. & Shahandi, M. R. Cretaceous tertiary convergence and continental collision. Sanandaj-Sirjan zone, western Iran. *J. Asian Earth Sci. v*. **21**, 397–412 (2003).
51. Chiu, H. Y. et al. Zircon Hf isotopic constraints on magmatic and tectonic evolution in Iran: implications for crustal growth in the Tethyan orogenic belt. *J. Asian Earth Sci. v*. **145**, 652–669. https://doi.org/10.1016/j.jseaes.2017.06.011 (2017).
52. Moghadam, H. S. et al. Crustal evolution of NW Iran: Cadomian arcs, Archean fragments and the cenozoic magmatic flare-up. *J. Petrol. v*. **58** (11), 2143–2190. https://doi.org/10.1093/petrology/egy005 (2017b).

53. Berberian, M. & King, G. C. P. Towards a paleogeography and tectonic evolution of Iran: Canadian Journal of Earth sciences, v. 18, pp. 210–265, (1981). https://doi.org/10.1139/e81-019
54. Agard, P., Omrani, J., Jolivet, L. & Mouthereau, F. Convergence history across Zagros (Iran): constraints from collisional and earlier deformation. *Int. J. Earth Sci. v.* **94**, 401–419. https://doi.org/10.1007/s00531-005-0481-4 (2005).
55. Azizi, H., Tanaka, T., Asahara, Y., Chung, S. L. & Zarrinkoub, M. H. Discrimination of the age and tectonic setting for magmatic rocks along the Zagros thrust zone, northwest Iran, using the zircon U–Pb age and Sr–Nd isotopes: Journal of Geodynamics, v. 52, pp. 304–320, (2011). https://doi.org/10.1016/j.jog.2011.03.001
56. Sheikholeslami, M. R. Evolution structurale et métamorphique de la marge sud de la microplaque de l'Iran central: les complexes métamorphiques de la région de Neyriz (Zone de Sanandaj- Sirjan) [Ph.D. thesis]: Brest, France, Université de Brest, p.194. (2002).
57. Moghadam, H. S. et al. Subduction, high-P metamorphism, and collision fingerprints in South Iran: constraints from zircon U–Pb and mica Rb–Sr geochronology. Geochemistry, Geophysics, Geosystems, v. 18, pp. 306–332, (2017). https://doi.org/10.1002/2016GC006585
58. Pandolfi, L. et al. The Bajgan Complex revealed as a cretaceous ophiolite-bearing subduction complex: a key to unravel the geodynamics of Makran (Southeast Iran). *J. Asian Earth Sci.* **222**, 104965. https://doi.org/10.1016/j.jseaes.2021.104965 (2021).
59. Monie, P. & Agard, P. Coeval blueschist exhumation along thousands of kilometers: implications for subduction channel processes. *Geochem. Geophys. Geosyst.* **10** (7). https://doi.org/10.1029/2009GC002428 (2009).
60. Sabzehei, M. Les melange ophiolitiques de la region de'Esfandagheh, These d'etate, Universite Scientifique et Medicale de Grenoble, France, p. 306. (1974).
61. Esmaeili, R. et al. S., Reconstructing the source and growth of the Makran Accretionary Complex: constraints from detrital zircon U-Pb geochronology, tectonics, **39**, e2019TC005963. (2020). https://doi.org/10.1029/2019TC005963
62. Shahabpour, J. Tectonic evolution of the orogenic belt in the region located between Kerman and Neyriz. *J. Asian Earth Sci. v.* **24**, 405–417 (2005).
63. Emami, M. H. Magmatism in Iran [in Persian]: Tehran, Geological Survey of Iran, 608 p. (2000).
64. James, G. A. & Wynd, J. G. *Stratigraphic Nomenclature of Iranian oil Consortium Agreement area*v. 49p. 2182–2245 (American Association of Petroleum Geologists Bulletin, 1965).
65. Sabzehei, M. et al. Geological map of the Neyriz quadrangle: Geological Survey of Iran, scale 1: 250,000, sheet H-11. (1993).
66. Afghah, M. & Farhoudi, G. Boundary between Upper Cretaceous and lower paleocene in the Zagros Mountain Ranges of Southwestern Iran: Acta Geologica Sinica, v. 86, 2, pp. 325–338, (2012). https://doi.org/10.1111/j.1755-6724.2012.00663.x
67. Piryaei, A., Reijmer, J. J. G., Borgomano, J. & Van Buchem, F. S. P. Late cretaceous tectonic and sedimentary evolution of the bandar Abbas area, fars region, southern Iran. *J. Petrol. Geol. v.* **34** (2), 157–180 (2011).
68. Piryaei, A. & Davies, R. B. Petroleum geology of the cenozoic succession in the Zagros of SW Iran: A sequence stratigraphic approach. *J. Petroleum Geol. v.* **47** (3), 1–56 (2024).
69. Motiei, H. Stratigraphy of Zagros: Internal Report [in Persian]: Tehran, Iran, Geological Survey of Iran, p. 572. (1993).
70. Hessami, K. H., Koyi, A., Talbot, C. J., Tabasi, H. & Shabanian, E. Progressive unconformities within an evolving foreland fold-thrust belt. *Zagros Mountains: J. Geol. Soc. Lond. v.* **158**, 969–981 (2001).
71. Daneshian, J., Derakhshani, M. & Moallemi, S. A. Relative age determination of Mishan formation deposits based on Foraminifera and Strontium isotope in the northwest and west of Bandar Abbas, south of Iran. *Strat Sediment. Res. V.* **32**, 35–54 (2016). (in Persian with English abstract)).
72. Seiffory Pour, S. Geological map of the Haji Abad: Geological Survey of Iran, scale 1: 100,000, sheet 7346. (2002).
73. Homke, S., Verges, J., Graces, M., Emami, H. & Karpuz, R. Magnetostratigraphy of Miocene–Pliocene Zagros foreland deposits in the front of the Push-e Kush Arc, (Lurestan Province, Iran): Earth and Planetary Science Letters, v. 225, p. 397. (2004).
74. Lanphere, M. A. & Pamic, J. 40Ar/39Ar ages and tectonic setting of ophiolite from the Neyriz area, southeast Zagros Range, Iran: Tectonophysics, v. 96, pp. 245–256, (1983). https://doi.org/10.1016/0040- 1951(83)90220-2.
75. Moghadam, H. S. & Stern, R. J. Geodynamic evolution of Upper cretaceous Zagros ophiolites: formation of oceanic lithosphere above a nascent subduction zone: Geological Magazine, v. 148, pp. 762–801, (2011). https://doi.org/10.1017/S0016756811000410
76. Monsef, I. et al. Evidence for an early-MORB to fore-arc evolution within the Zagros suture zone: constraints from zircon U-Pb geochronology and geochemistry of the Neyriz ophiolite (south Iran): Gondwana Research, v. 62, pp. 287–305, (2018). https://doi.org/10.1016/j.gr.2018.03.002
77. Hacker, B. R. Rapid emplacement of young oceanic lithosphere: Argon geochronology of the Oman ophiolite: Science, v. 265, pp. 1563– 1565. (1994).
78. Hacker, B. R. & Mosenfelder, J. L. Metamorphism and deformation along the emplacement thrust of the Samail ophiolite, Oman: Earth Planet. *Sci. Lett. v.* **144**, 435–451 (1996).
79. Rioux, M. et al. Synchronous formation of the metamorphic sole and igneous crust of the Semail ophiolite: new constraints on the tectonic evolution during ophiolite formation from high-precision U-Pb zircon geochronology, Earth and Planetary Science letters, v. 451, pp. 185–195. (2016). https://doi.org/10.1016/j.epsl.2016.06.051
80. Sabzehei, M. et al. (1994). Geological map of the Haji Abad quadrangle: Geological Survey of Iran, scale 1: 250,000.
81. Sepidbar, F., Zaki Khedr, M., Ghorbani, M. R., Palin, R. M. & Xiao, Y. *Petrogenesis of arc-related Peridotite Hosted Chromitite Deposits in Sikhoran-Soghan Mantle Section, South Iran: Evidence for proto-forearc Spreading to Boninitic Stages*v. 136104256 (Ore Geology Reviews, 2021).
82. Ghasemi, H. et al. *The mafic-ultramafic Complex of Sikhoran (Central Iran): A Polygenetic Ophiolite Complex*v. 334p. 431–438 (C. R. Geoscience, 2002).
83. Ahmadipour, H., Sabzehi, M., Whitechurch, H., Rastad, E. & Emami, M. H. Soghan complex as an evidence for paleospreading center and mantle diapirism in Sanandaj–Sirjan Zone (south-east Iran): Journal of sciences, Islamic Republic of Iran v. 14, pp. 157–172. (2003).
84. Moghadam, H. S., Mosaddegh, H. & Santosh, M. Geochemistry and petrogenesis of the late cretaceous Haji-Abad ophiolite (outer Zagros Ophiolite Belt, Iran): implications for geodynamics of the Bitlis–Zagros suture zone: Geological Journal, v. 48, pp. 579–602, (2013). https://doi.org/10.1002/gj.2458
85. Moghadam, H. S. et al. Chemostratigraphy of the extrusive sequence of a late cretaceous neotethyan ophiolite in southern Iran and its significance for the mode and tempo of subduction initiation magmatism and melt evolution in forearc tectonic settings. *J. Geol. Soc.* **180**, 80. https://doi.org/10.1144/jgs2023-080 (2023).
86. Mohammadi, M., Ahmadipour, H. & Moradian, A. Origin of Lherzolitic peridotites in Ab-Bid Ultramafic Complex (Hormozgan Province); products of Mantle Metasomatism or partial melting processes? *J. Sci. Islamic Repub. Iran. v.* **29** (1), 53–65 (2018).
87. Delavari, M., Dolati, A., Marroni, M., Pandolfi, L. & Saccani, E. Association of MORB and SSZ ophiolites along the shear zone between Coloured M´elange and Bajgan Complexes (North Maran, Iran): evidence from the Sorkhband area: Ofioliti v. **41**, pp. 21–34. (2016).
88. Ingersoll, R. V. et al. The effect of grain size on detrital modes: a test of the Gazzi Dickinson point-counting method. *J. Sediment. Petrol. v.* **54**, 103–116 (1984).
89. Zuffa, G. G. Optical analyses of arenites: influence of methodology on compositional results. In: Zuffa, G.G. (Ed.), Provenance of Arenites, NATO-ASI Series 148, pp. 165–189. (1985).
90. Garzanti, E. & Vezzoli, G. A classification of metamorphic grains in sands based on their composition and grade. *J. Sediment. Res. v.* **73** (5), 830–837 (2003).

91. Critelli, S., Criniti, S., Ingersoll, R. V. & Cavazza, W. Temporal and Spatial significance of volcanic particles in sand (stone): implications for provenance and paleotectonics, in Di Capua, A., De Rosa, R., Kereszturi, G., Le Pera, E., Rosi, M. and Watt, S. F.L., eds., Volcanic Processes in the Sedimentary Record: When Volcanoes Meet the Environment: Geological Society of London Special Publication 520, pp. 311–325, (2023). https://doi.org/10.1144/SP520-2022-99
92. Perrotta, S. et al. Detrital signatures of clastic serpentinite in tectonically diverse settings and interpretation of an example from the Northern Apennines. *J. Sediment. Res. v*. **94** (3), 207–230. https://doi.org/10.2110/jsr.2022.093 (2024).
93. Garzanti, E. From static to dynamic provenance analysis—sedimentary petrology upgraded: sedimentary geology, v. 336, pp. 3–13, (2016). https://doi.org/10.1016/j.sedgeo.2015.07.010
94. e4 Garzanti, E. Petrographic classification of sand and sandstone: Earth-Science Reviews, v. 192, pp. 545–563, (2019). https://doi.org/10.1016/j.earscirev.2018.12.014
95. Paton, C. et al. Improved laser ablation U-Pb zircon geochronology through robust downhole fractionation correction: Geochem. *Geophys. Geosyst.* **11**, 3 (2010).
96. Vermeesch, P. On the visualisation of detrital age distributions. *Chem. Geol. v*. **313**, 312 (2012).
97. Vervoort, J. D., Patchett, P. J., Soderlund, U. & Baker, M. Isotopic composition of Yb and the determination of Lu concentrations and Lu/Hf ratios by isotope dilution using MC-ICPMS. *Geochem. Geophys. Geosyst.* **5**, Q11002. https://doi.org/10.1029/2004GC000721 (2004).
98. Wu, F., Wan, B., Zhao, L., Xiao, W. & Zhu, R. Tethyan geodynamics: Acta Petrologica 910: Sinica, v. 36, pp. 1627–1674. (2020).
99. Xie, L. W., Zhang, Y. B., Zhang, H. H., Sun, J. F. & Wu, F. Y. In situ simultaneous determination of trace elements, U-Pb and Lu-Hf isotopes in zircon and baddeleyite. *Chin. Sci. Bull. v*. **53**, 1565–1573 (2008).
100. Huang, C. et al. In-run measuring 177Hf16O/177Hf as a routine technique for in-situ hf isotopic compositions analysis in zirconium-bearing minerals by laser ablation MC-ICP-MS. *Spectrochimica Acta Part. B: at. Spectrosc.* **194**, 106486 (2022).
101. Ezampanah, Y., Di Lucia, M., Yazdi-Moghadam, M. & Zaghbib-Turki, D. Planktonic foraminiferal distribution of the late cretaceous to late Paleocene deposits of the Bandar Abbas area (Zagros Belt, SW Iran): an update of the bio- and lithostratigraphic framework. *J. Afr. Earth Sc.* **185**, 104392 (2022).
102. Orang, K., Hossein, M., Azadikhah, A. & Royatvand, M. Structural framework and tectono-stratigraphic evolution of the Easten Persian Gulf, offshore Iran: Mar. Petrol. *Geol. v*. **91**, 89–107. https://doi.org/10.1016/j.marpetgeo.2017.12.014 (2017).
103. Gholamalian, H., Rameshgar, R., Sharif-Abad, L. & Aziz, F. M., Microbiostratigraphy of Miocene Guri Member of the Mishan formation in the Bandar Abbas area, SE Zagros, Iran: carbonates and evaporites, **38**:17 (2023). https://doi.org/10.1007/s13146-022-00843-9
104. Garzanti, E., Vezzoli, G. & Ando, S. Modern sand from obducted ophiolite belts (Sultanate of Oman and United Arab Emirates). *J. Geol. v*. **110** (4), 371–391 (2002).
105. Grimes, C. B., Wooden, J. L., Cheadle, M. J. & John, B. E. Fingerprinting tectono-magmatic provenance using trace elements in igneous zircon. *Contrib. Miner. Petrol.* **170** (5), 1–26. https://doi.org/10.1007/s00410-015-1199-3 (2015).
106. Taraz, H. Géologie de la Région de Surmaq-Deh-Bid (Central Iran) [Ph.D. thesis]: Orsay, France, Université de Paris-Sud, p.148. (1972).
107. Houshmandzadeh, A. Explanatory text of the Eqlid quadrangle map: Geological Survey of Iran, G10, scale 1:250,000, 158 p. (1990).
108. Jahani, S., Callot, J. P., Frizon de Lamotte, D., Letouzey, J. & Leturmy, P. The salt diapirs of the eastern Fars province (Zagros, Iran): a brief outline of their past and present. In: (eds Lacombe, O., Lav`e, J., Roure, F. & Verg`es, J.) Thrust Belts and Foreland Basins. Springer, Berlin, 289–308. https://doi.org/10.1007/978-3-540-69426-7_15. (2007).
109. Horton, B. K. et al. Detrital zircon provenance of neoproterozoic to cenozoic deposits in Iran: implications for chronostratigraphy and collisional tectonics: tectonophysics, v. 451, pp. 97–122, (2008). https://doi.org/10.1016/j.tecto.2007.11.063
110. Faramarzi, N. S. et al. Geochronology and geochemistry of rhyolites from Hormuz Island, southern Iran: a new record of cadomian arc magmatism in the Hormuz formation: eLithos, v. 236, pp. 203–211. (2015). https://doi.org/10.1016/j. lithos.2015.08.017
111. Bowring, S. A. et al. Geochronologic constraints on the chronostratigraphic framework of the neoproterozoic huqf supergroup, Sultanate of Oman: am. *J. Sci. v*. **307** (10), 1097–1145. https://doi.org/10.2475/10.2007.01 (2007).
112. Moghadam, H. S. et al. Cadomian (Ediacaran–Cambrian) arc magmatism in the ChahJam–Biarjmand metamorphic complex (Iran): magmatism along the northern active margin of Gondwana. *Gondwana Res. V*. **27** (1), 439–452 (2015).
113. Zohdi, A., Moallemi, S. A., Mousavi Harami, R., Mahboubi, A. & Nikandish, A. A. Paleo-ecology, evolution of sedimentary environment and sequence stratigraphy of the Jahrum Formation in the Bandar-Abbas Region (SE ZagrosBasin). 7th Conference of Iranian Paloontological Society, Iran. (2013).
114. Ballato, P. et al. *Arabia- Eurasia Continental Collision: Insights from late Tertiary foreland-basin Evolution in the Alborz Mountains, Northern Iran*v.123p.106–131 (Geological Society of America Bulletin, 2011). no.1–210.1130/B30091.1
115. Molinaro, M., Leturmy, P., Guezou, J. C., De Lamotte, F. & Eshraghi, S. A. D., and The structure and kinematics of the southeastern Zagros fold-thrust belt, Iran: from thin-skinned to thick-skinned tectonics: tectonics, v. 24, no. TC3007, (2005). https://doi.org/10.1029/2004TC001633
116. Daneshian, J., Derakhshani, M. & Moallemi, S. A. Study of Foraminifera of the Mishan formation in Handun section in Northwest Bandar Abbas and its application in sequence stratigraphy: Adv Appl Geol v. 23, pp. 29–41 (2017). (in Persian with English abstract)).
117. Michaelis, P. L. & Pauken, R. J. *Seismic Interpretation of the Structure and Stratigraphy of the Strait of Hormuz*v. 49p. 387–395 (Geological Society of London, Special Publication, 1990).
118. Heidari, A., Mahboubi, A., Moussavi-Harami, R., Gonzalez, L. & Moallemi, S. A. Biostratigraphy, sequence stratigraphy, and paleoecology of the Lower–Middle Miocene of Northern Bandar Abbas, Southeast Zagros basin in south of Iran. *Arab. J. Geosci.* **7**, 1829–1855. https://doi.org/10.1007/s12517-012-0803-3 (2014).
119. Decelles, P. G., Kapp, P., Gehrels, G. E. & Ding, L. Paleocene-Eocene foreland basin evolution in the Himalaya of southern Tibet and Nepal: implications for the age of initial India-Asia collision: tectonics, v. 33, pp. 824–849. (2014). https://doi.org/10.1002/2014TC003522
120. Garzanti, E. et al. Tracing Transcontinental Sand Transport: from Anatolia–Zagros to the rub'Al Khali Sand Sea. *J. Sediment. Res. v*. **87** (11), 1196–1213 (2017).
121. Ezati Asl, M., Faghih, A., Mukherjee, S. & Soleimany, B. Style and timing of salt movement in the Persian Gulf basin, offshore Iran: insights from halokinetic sequences adjacent to the Tonb-e-Bozorg salt diaper. *J. Struct. Geol. v*. **122**, 116–132. https://doi.org/10.1016/j.jsg.2019.02.002 (2019).
122. Snidero, M. et al. Diapir kinematics in a multi-layer salt system from the eastern Persian Gulf. *Mar. Pet. Geol.* 117. https://doi.org/10.1016/j. marpetgeo.2020.104402 (2020).
123. Ali, M. Y., Aidarbayev, S., Searle, M. P. & Watts, A. B. Subsidence history and seismic stratigraphy of the western Musandam Peninsula, Oman–United Arab Emirates mountains. *Tectonics* **37**, 154–181. https://doi.org/10.1002/2017TC004777 (2018).
124. Sahandi, M. R. & Soheili, M. *Geological Map of Iran, Scale 1:1000000* (Geological Survey of Iran, 2014).
125. McCall, G. J. H. Explanatory text of the Minab quadrangle map 1:250,000, Geol. (1985). Surv. of Iran, Geological Quadrangle, No. J 13.
126. Griffin, W. L. et al. The hf isotope composition of cratonic mantle: LAM-MC-ICPMS analysis of zircon megacrysts in kimberlites. *Geochim. et Cosmochim. Acta v*. **64** (1), 133–147 (2000).

Acknowledgements
This research was supported by NSFC 92255303 and the Geological Survey of Iran. The authors would like to express their gratitude to Prof. F. Wu, Dr. (A) Piryaei and Mr. S.A. Eshraghi for their invaluable discussions. Special thanks are extended to Zhiyong Zhang for his useful suggestions and assistance in organizing laboratory work, as well as to W. Zhang and Sh. Wang for their contributions during Hf isotope analysis. We also appreciate Mojgan Zare for helping with paleontological determinations. The first author is grateful for support from IGG-CAS postdoctoral program (2016IFPR01) under the guidance of Prof. (B) Wan. Finally, we would like to express our appreciation to the three reviewers, Michele Marroni, William Cavazza, and Salvatore Critelli for providing insightful comments and suggestions, and Alakananda Karthick, Editorial Board Member, for her valuable comments and for managing the manuscript.

Author contributions
Parisa GholamiZadeh: Writing – original draft, review and editing, Conceptualization, data Curation. Bo Wan: Conceptualization, Review and editing, Funding acquisition. Eduardo Garzanti: Writing – review and editing, Conceptualization. Xiumian Hu: Conceptualization, Review and editing. Rasoul Esmaeili: Data curation. Mohammad Ebrahimi: Data curation. All authors discussed and contributed to the publication.

Competing interests
The authors declare no competing interests.

Additional information
Supplementary Information The online version contains supplementary material available at https://doi.org/10.1038/s41598-025-90186-x.

Correspondence and requests for materials should be addressed to P.G.